CHEMISTRY
A EUROPEAN JOURNAL

DOI: 10.1002/chem.200800492

Half-Sandwich Bis(tetramethylaluminate) Complexes of the Rare-Earth Metals: Synthesis, Structural Chemistry, and Performance in Isoprene Polymerization

Melanie Zimmermann,[a] Karl W. Törnroos,[a] Helmut Sitzmann,[b] and Reiner Anwander*[a]

Abstract: The protonolysis reaction of $[Ln(AlMe_4)_3]$ with various substituted cyclopentadienyl derivatives HCp^R gives access to a series of half-sandwich complexes $[Ln(AlMe_4)_2(Cp^R)]$. Whereas bis(tetramethylaluminate) complexes with $[1,3\text{-}(Me_3Si)_2C_5H_3]$ and $[C_5Me_4SiMe_3]$ ancillary ligands form easily at ambient temperature for the entire Ln^{III} cation size range (Ln = Lu, Y, Sm, Nd, La), exchange with the less reactive $[1,2,4\text{-}(Me_3C)_3C_5H_3]$ was only obtained at elevated temperatures and for the larger metal centers Sm, Nd, and La. X-ray structure analyses of seven representative complexes of the type $[Ln(AlMe_4)_2(Cp^R)]$ reveal a similar distinct $[AlMe_4]$ coordination (one η^2, one bent η^2). Treatment with Me_2AlCl leads to $[AlMe_4] \rightarrow [Cl]$ exchange and, depending on the Al/Ln ratio and the Cp^R ligand, varying amounts of partially and fully exchanged products $[\{Ln(AlMe_4)(\mu\text{-}Cl)(Cp^R)\}_2]$ and $[\{Ln(\mu\text{-}Cl)_2(Cp^R)\}_n]$, respectively, have been identified. Complexes $[\{Y(AlMe_4)(\mu\text{-}Cl)(C_5Me_4SiMe_3)\}_2]$ and $[\{Nd(AlMe_4)(\mu\text{-}Cl)\{1,2,4\text{-}(Me_3C)_3C_5H_2\}\}_2]$ have been characterized by X-ray structure analysis. All of the chlorinated half-sandwich complexes are inactive in isoprene polymerization. However, activation of the complexes $[Ln(AlMe_4)_2(Cp^R)]$ with boron-containing cocatalysts, such as $[Ph_3C][B(C_6F_5)_4]$, $[PhNMe_2H][B(C_6F_5)_4]$, or $B(C_6F_5)_3$, produces initiators for the fabrication of *trans*-1,4-polyisoprene. The choice of rare-earth metal cation size, Cp^R ancillary ligand, and type of boron cocatalyst crucially affects the polymerization performance, including activity, catalyst efficiency, living character, and polymer stereoregularity. The highest stereoselectivities were observed for the precatalyst/cocatalyst systems $[La(AlMe_4)_2(C_5Me_4SiMe_3)]/B(C_6F_5)_3$ (*trans*-1,4 content: 95.6%, $M_w/M_n = 1.26$) and $[La(AlMe_4)_2(C_5Me_5)]/B(C_6F_5)_3$ (*trans*-1,4 content: 99.5%, $M_w/M_n = 1.18$).

Keywords: aluminum · boron · cyclopentadienyl ligands · isoprene · lanthanides · polymerization

Introduction

Bis(alkyl) complexes of the type $[Ln^{III}(Do)(\mathbf{L})R_2]$ bearing a monoanionic ancillary ligand ($\mathbf{L}^-$) (R = CH_2SiMe_3, $CH_2Ph^{R'}$; Do = neutral donor ligand) have proved to be extremely versatile catalyst precursors in organolanthanide-promoted polymerization reactions.[1–5] In particular, Hou and Okuda noted a remarkable performance of these discrete complexes in catalytic polymerizations of styrene and 1,3-diene following cationization with borate activators.[1b,e,f,g,2e,4a] Pivotal structure–reactivity relationships revealed specific effects of the Ln^{III} cation size and the nature of the ancillary ligand ($\mathbf{L}^-$) on the performance in polymerization, including activity, efficiency, living character, and polymer stereoregularity.[1b,2e,4a,6] For example, the cationic complex $[Y(CH_2SiMe_3)(C_5Me_4SiMe_3)(thf)][B(C_6F_5)_4]$ has been reported to act as a highly efficient initiator for the syndiospecific polymerization of styrene (>99% *syndio*; $M_w/M_n = 1.39$),[1b] while it showed only poor selectivity in the polymerization of isoprene (66% 3,4-; $M_w/M_n = 1.06$).[6] On the other hand, complexes $[Ln(CH_2SiMe_3)(PNP^{Ph})(thf)_2][B(C_6F_5)_4]$ ($PNP^{Ph} = [\{2\text{-}(Ph_2P)C_6H_4\}_2N]$; Ln = Sc, Y, Lu) bearing an amido ancillary ligand afforded high *cis*-1,4 selectivity and "livingness" in the polymerization of isoprene in the absence of any aluminum additive (>99% *cis*-1,4; $M_w/M_n = 1.05$).[4a]

[a] Dr. M. Zimmermann, Prof. Dr. K. W. Törnroos, Prof. Dr. R. Anwander
Department of Chemistry, University of Bergen
Allégaten 41, 5007 Bergen (Norway)
Fax: (+47) 5558-9490
E-mail: reiner.anwander@kj.uib.no

[b] Prof. Dr. H. Sitzmann
FB Chemie, Technische Universität Kaiserslautern
Erwin-Schrödinger-Straße 52, 67633 Kaiserslautern (Germany)

We have recently introduced half-sandwich bis(tetramethylaluminate) rare-earth metal complexes of the type [Ln^{III}-$(AlMe_4)_2$(**L**)] (**L** = C_5Me_5) as alternative bis(hydrocarbyl) derivatives.[7,8] The reactivity pattern of such alkylaluminate complexes is consistent with their formulation as "alkyls in disguise", that is, [$Ln^{III}(AlMe_3)_2Me_2$(**L**)]. Their most striking features are: a) availability for the entire Ln^{III} cation size range;[9] b) accessibility by versatile synthesis protocols comprising both protonolysis and salt metathesis approaches;[7,8,10] c) enhanced thermal stability (e.g., [Ln-$(AlMe_4)_2(C_5Me_5)$] may be sublimed) and hence suitability for storage;[11] d) coordinational flexibility of the [$AlMe_4$] ligands, as evidenced by $\eta^{1/2/3}$ coordination modes;[9,12–14] e) an absence of coordinating donor molecules (Do);[15] and f) the presence of $AlMe_3$ as an internal solvent scavenger.[16] Moreover, our previous work highlighted the pivotal role of heterobimetallic [Ln(μ-R)$_n$Al] moieties in the activation of rare-earth metal-based Ziegler-type catalysts.[17–20] Based on these mechanistic insights and the favorable chemical and structural features of alkylaluminate ligands, we set out to develop a bis(tetramethylaluminate) postmetallocene library, considering carbocyclic (e.g., cyclopentadienyl),[7,8] heterocyclic (e.g., phosphacyclopentadienyl),[10] *N*-donor (e.g., amido),[13,21] as well as *O*-donor (e.g., alkoxo) ancillary ligands **L** (Figure 1).[20] The aim of creating this postmetallocene library is to gain a fundamental understanding of ancillary ligand and cocatalyst effects, and hence to elucidate the structure–reactivity relationships in non-metallocene polymerization catalysis.

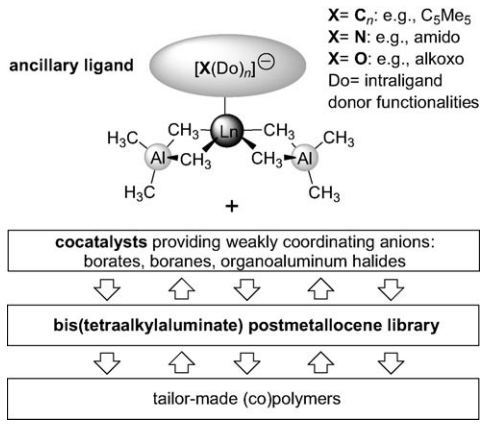

Figure 1. Rare-earth metal-based bis(tetraalkylaluminate) postmetallocene library.

Recently, we reported the remarkable potential of [Ln-$(AlMe_4)_2(C_5Me_5)$] to initiate the living *trans*-1,4 stereospecific polymerization of isoprene (*trans*-1,4 selectivity up to 99.5%), and hence the fabrication of synthetic guttapercha.[22] Herein, we present a more comprehensive account of the synthesis and structural chemistry of half-sandwich complexes [$Ln(AlMe_4)_2(Cp^R)$] containing various substituted cyclopentadienyl ancillary ligands.[23] Special emphasis is placed on their catalytic performance in the polymerization of isoprene, considering precatalyst–cocatalyst interactions and structure–reactivity relationships.

Results and Discussion

Synthesis and structural chemistry of half-sandwich bis(tetramethylaluminate) complexes [Ln$(AlMe_4)_2(Cp^R)$]: Protonolysis of homoleptic [$Ln(AlMe_4)_3$] complexes (Ln = Lu (**1a**), Y (**1b**), Sm (**1c**), Nd (**1d**), and La (**1e**))[9] with one equivalent of substituted HCp^R (Cp^R = [1,3-$(Me_3Si)_2C_5H_3$][24] and [$C_5Me_4SiMe_3$]) in hexane at ambient temperature yielded the corresponding bis(tetramethylaluminate) complexes [$Ln(AlMe_4)_2(Cp^R)$] (**2** and **3**) in quantitative yields (Scheme 1).[25] Instant gas evolution evidenced the anticipated methane elimination reaction, and hence the immediate acid-base reaction of [$Ln(AlMe_4)_3$] and the respective substituted cyclopentadiene. (CAUTION: volatiles containing trimethylaluminum react violently when exposed to air).

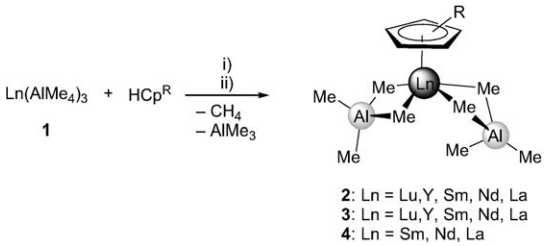

Scheme 1. Synthesis of [$Ln(AlMe_4)_2(Cp^R)$]: i) hexane, 5 h, RT, (Ln = Lu, Cp^R = [1,3-$(Me_3Si)_2C_5H_3$] (**2a**); Ln = Y, Cp^R = [1,3-$(Me_3Si)_2C_5H_3$] (**2b**); Ln = Sm, Cp^R = [1,3-$(Me_3Si)_2C_5H_3$] (**2c**); Ln = Nd, Cp^R = [1,3-$(Me_3Si)_2C_5H_3$] (**2d**); Ln = La, Cp^R = [1,3-$(Me_3Si)_2C_5H_3$] (**2e**); Ln = Lu, Cp^R = [$C_5Me_4SiMe_3$] (**3a**); Ln = Y, Cp^R = [$C_5Me_4SiMe_3$] (**3b**); Ln = Sm, Cp^R = [$C_5Me_4SiMe_3$] (**3c**); Ln = Nd, Cp^R = [$C_5Me_4SiMe_3$] (**3d**); Ln = La, Cp^R = [$C_5Me_4SiMe_3$] (**3e**)); ii) toluene, 24 h, 100 °C (Ln = Sm, Cp^R = [1,2,4-$(Me_3C)_3C_5H_2$] (**4c**); Ln = Nd, Cp^R = [1,2,4-$(Me_3C)_3C_5H_2$] (**4d**); Ln = La, Cp^R = [1,2,4-$(Me_3C)_3C_5H_2$] (**4e**)).

Attempts to prepare half-sandwich derivatives containing the sterically demanding and electronically deactivated [1,2,4-$(Me_3C)_3C_5H_2$] ligand by the same procedure were unsuccessful.[26] However, heating [$Ln(AlMe_4)_3$] (Ln = Sm (**1c**), Nd (**1d**), La (**1e**)) with one equivalent of [1,2,4-$(Me_3C)_3C_5H_3$] in toluene at 100 °C for 24 h resulted in the formation of [$Ln(AlMe_4)_2${1,2,4-$(Me_3C)_3C_5H_2$}] (**4**) in good yields (Scheme 1). Nevertheless, the availability of complexes **4** bearing such bulky cyclopentadienyl ligands seems to be limited to the large lanthanide metal centers (Ln = Sm, Nd, La). It is noteworthy that the formation of [Sm-$(AlMe_4)_2${1,2,4-$(Me_3C)_3C_5H_2$}] (**4c**) is accompanied by the precipitation of an insoluble purple solid. Characterization of this precipitate revealed it to be peralkylated divalent [$SmAl_2Me_8]_n$.[27] Donor adduct formation in the presence of THF yielded [$SmAl_2Me_8(thf)_2$], further substantiating the reduction of the samarium metal center ($Sm^{III} \rightarrow Sm^{II}$).[28] However, the observed reactivity has not been investigated further.

The ^{1}H NMR spectra of diamagnetic mono(cyclopentadienyl) complexes **2**–**4** (Ln = Lu, Y, La) show the expected sets of signals for the respective Cp^R ligands and only one narrow signal in the metal alkyl region, which can be assigned to the $[Al(\mu\text{-}Me)_2Me_2]$ moieties, indicating a rapid exchange of bridging and terminal methyl groups. For compounds **2** and **3**, these resonances are slightly shifted to higher field compared to those of the homoleptic precursors,[9] while a downfield shift is observed for compound **4e** (Table 1). A signal splitting of the ^{1}H methyl resonance in yttrium compounds **2b** ($^2J_{YH}$ = 2.4 Hz) and **3b** ($^2J_{YH}$ = 2.0 Hz) is clearly attributable to a two-bond ^{1}H-^{89}Y scalar coupling.

Good quality ^{1}H and ^{13}C NMR spectra could also be obtained for the paramagnetic compounds $[Sm(AlMe_4)_2(Cp^R)]$ (**2c**, **3c**, **4c**) and $[Nd(AlMe_4)_2(Cp^R)]$ (**2d**, **3d**, **4d**). The paramagnetic Ln^{III} metal centers influence the ^{1}H and ^{13}C NMR spectra differently, probably due to the varying relaxation behavior of their unpaired electron spins. Significant paramagnetic shifts and broadening effects for the ^{1}H and ^{13}C resonances are observed for complexes containing neodymium, while such effects are less pronounced for the respective samarium compounds (Table 1).

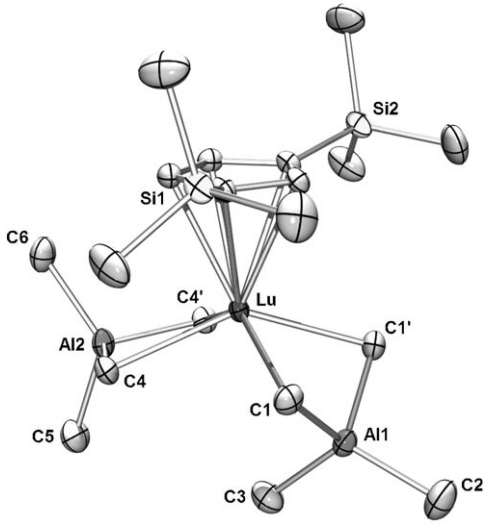

Figure 2. Molecular structure of $[Lu(AlMe_4)_2\{1,3\text{-}(Me_3Si)_2C_5H_3\}]$ (**2a**), representative of isostructural complexes **2**; atomic displacement parameters are set at the 50% level; hydrogen atoms have been omitted for clarity; symmetry code for (′) is x, $3/2-y$, z.

Table 1. ^{1}H NMR chemical shifts (ppm) of the $[Al(CH_3)_4]$ protons of tetramethylaluminate-containing complexes. Values are taken from ^{1}H NMR spectra of the respective compounds dissolved in $[D_6]$benzene at 298 K.

	Lu	Y	Sm	Nd	La
$[Ln(AlMe_4)_3]$ (**1**)[a]	−0.08	−0.25	−3.06	10.53	−0.20
$[Ln(AlMe_4)_2\{1,3\text{-}(Me_3Si)_2C_5H_3\}]$ (**2**)	−0.14	−0.29	−2.81	6.78	−0.23
$[Ln(AlMe_4)_2(C_5Me_4SiMe_3)]$ (**3**)	−0.14	−0.31	−3.14	5.25	−0.25
$[Ln(AlMe_4)_2\{1,2,4\text{-}(Me_3C)_3C_5H_2\}]$ (**4**)	–	–	−2.76	6.40	−0.12
$[Ln(AlMe_4)_2(C_5Me_5)]$ (**5**)[b]	−0.18	−0.33	−3.27	4.21	−0.27
$[\{Ln(AlMe_4)(\mu\text{-}Cl)\{1,3\text{-}(Me_3Si)_2C_5H_3\}\}_2]$ (**6**)	–	−0.11	–	–	–
$[\{Ln(AlMe_4)(\mu\text{-}Cl)(C_5Me_4SiMe_3)\}_2]$ (**8**)	–	−0.20	–	–	–
$[\{Ln(AlMe_4)(\mu\text{-}Cl)\{1,2,4\text{-}(Me_3C)_3C_5H_2\}\}_2]$ (**9**)	–	–	–	9.63	–
$[\{Ln(AlMe_4)(\mu\text{-}Cl)(C_5Me_5)\}_2]$[c]	–	−0.15	–	–	–
$[La(AlMe_4)(C_5Me_5)][B(C_6F_5)_4]$[d]					−0.39
$[\{[La(C_5Me_5)\{(\mu\text{-}Me)_2AlMe(C_6F_5)\}][Me_2Al(C_6F_5)_2]\}_2]$[d,e]					−0.24, −0.37

[a] Taken from ref. [9]. [b] Taken from refs. [7, 8, and 29]. [c] Taken from ref. [14]. [d] Taken from ref. [22]. [e] Chemical shifts for the bridging and terminal methyl groups of the $[(\mu\text{-}Me)_2AlMe(C_6F_5)]$ moiety.

Single crystals of $[Ln(AlMe_4)_2\{1,3\text{-}(Me_3Si)_2C_5H_3\}]$ (Ln = Lu (**2a**), Y (**2b**), Nd (**2d**)), $[Y(AlMe_4)_2(C_5Me_4SiMe_3)]$ (**3b**), and $[Ln(AlMe_4)_2\{1,2,4\text{-}(Me_3C)_3C_5H_2\}]$ (Ln = Sm (**4c**), Nd (**4d**), La (**4e**)) suitable for X-ray crystallographic structure determination were grown from saturated hexane solutions at −30 °C. This series covers the differently substituted cyclopentadienyl ligands as well as a wide size range of Ln^{III} cations, thus allowing an insight into the ligand- and size-dependent characteristics of complexes $[Ln(AlMe_4)_2(Cp^R)]$ in the solid state. The X-ray crystallographic analyses revealed structural motifs as previously found for $[Ln(AlMe_4)_2(C_5Me_5)]$ (Ln = Lu (**5a**), Y (**5b**), La (**5e**)), with one $[AlMe_4]$ ligand coordinating in the routinely observed planar η^2 fashion and the second one showing a bent η^2-coordination (Figures 2 and 3).[7,8,11]

All of the solid-state structures under investigation feature an additional short Ln···(μ-Me) contact (Ln···C3, **2**; Ln···C7, **3** and **4**). Due to enhanced steric unsaturation, this interaction becomes more distinct with increasing size of the lanthanide metal center, as is reflected in a gradual shortening of the (bond) distances Ln···C3 (**2**, Table 2) and Ln···C7 (**3** and **4**, Table 3), respectively.

This effect is, however, less pronounced for complexes **4**, as one might reasonably expect, due to effective stereoelectronic shielding by the bulky $[1,2,4\text{-}(Me_3C)_3C_5H_2]$ ligand. Interplanar angles LnC1C1′-Al1C1C1′ (**2**) and LnC5C6-Al2C5C6 (**3**, **4**) follow similar trends (**2a**: 128.5°, **2b**: 124.5°, **2d**: 117.7°; **3b**: 121.0°; **4c**: 126.8°, **4d**: 125.8°, **4e**: 124.0°). The Ln−C(μ-Me) bond lengths increase with increasing Ln^{III} size, the bonds in the bent $[AlMe_4]$ ligand being significantly elongated compared to those in the planar tetramethylaluminate ligand of the same molecule (Tables 2 and 3). To minimize steric hindrance, the orientation of the trimethylsilyl substituents at the cyclopentadienyl ring in compounds $[Ln(AlMe_4)_2\{1,3\text{-}(Me_3Si)_2C_5H_3\}]$ (**2**) is nearly staggered with respect to the two aluminate ligands (Figure 2). Due to the increased steric crowding in complexes $[Ln(AlMe_4)_2\{1,2,4\text{-}(Me_3C)_3C_5H_2\}]$ (**4**), the mean metal–ring-carbon distances Ln−C(1,2,4-$(Me_3C)_3C_5H_2$) are considerably elongated compared to those in $[Ln(AlMe_4)_2(C_5Me_5)]$ (**5**) (e.g., av. 2.807 Å in **4e** vs av. 2.777 Å in **5e**).[8] Steric repulsion leads

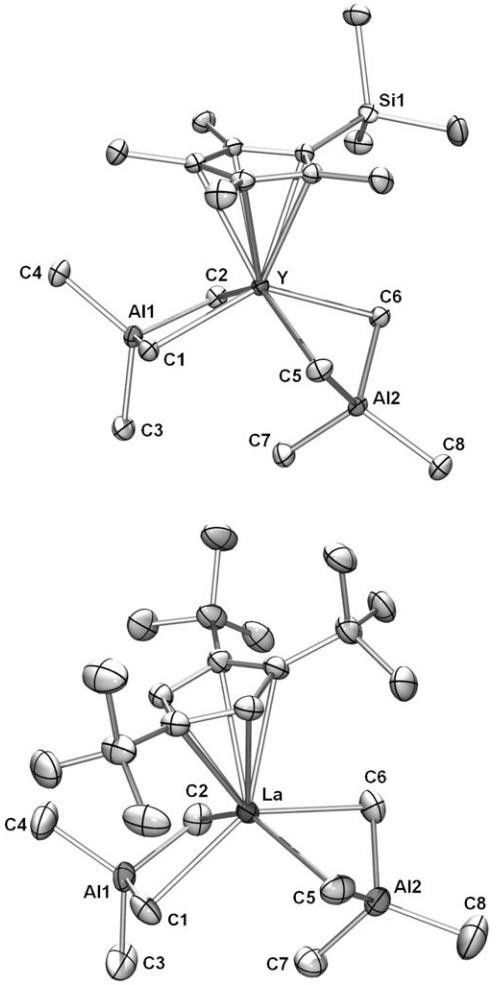

Figure 3. Molecular structures of $[Y(AlMe_4)_2(C_5Me_4SiMe_3)]$ (**3b**) (top) and $[La(AlMe_4)_2\{1,2,4\text{-}(Me_3C)_3C_5H_2\}]$ (**4e**) (bottom; representative of isostructural complexes **4**); atomic displacement parameters are set at the 50% level; hydrogen atoms have been omitted for clarity.

Table 2. Selected structural parameters [Å, °] for complexes **2a**, **2b**, and **2d** (C_g = ring centroid). Symmetry code for (′) depicts (x, 3/2−y, z).

	2a (Lu)	**2b** (Y)	**2d** (Nd)
Ln−C(Cp^R)	2.580(2)–2.596(1)	2.620(3)–2.641(2)	2.713(2)–2.727(1)
Ln−C_g	2.29	2.34	2.44
Ln−C1/C1′	2.563(1)	2.624(2)	2.731(2)
Ln−C4/C4′	2.517(1)	2.560(2)	2.645(2)
Al1−C1/C1′	2.069(1)	2.062(2)	2.057(2)
Al1−C2	1.959(2)	1.949(3)	1.957(2)
Al1−C3	1.974(2)	1.983(3)	2.012(2)
Al2−C4/C4′	2.082(2)	2.085(2)	2.084(2)
Al2−C5	1.971(2)	1.969(3)	1.973(2)
Al2−C6	1.971(2)	1.964(3)	1.971(2)
Ln···Al1	2.9130(5)	2.9133(9)	2.9498(6)
Ln···Al2	3.0292(5)	3.078(1)	3.1722(6)
Ln···C3	3.492(2)	3.302(3)	3.088(2)
C1-Ln-C1′	79.98(5)	78.2(1)	74.52(7)
C4-Ln-C4′	84.45(5)	83.3(1)	80.53(6)
Ln-C1-Al1	77.13(4)	75.8(1)	74.57(5)
Ln-C4-Al2	81.80(4)	82.31(7)	83.35(5)
C1-Al1-C1′	105.50(7)	106.8(1)	106.95(9)
C4-Al2-C4′	108.73(6)	109.4(1)	110.25(8)
C1′-Al1-C2	106.55(5)	108.0(1)	111.35(6)
C1′-Al1-C3	108.09(5)	106.06(9)	104.56(6)
C4′-Al2-C5	105.73(5)	105.89(9)	106.05(6)
C4-Al2-C6	109.59(4)	109.12(9)	109.32(6)
Al1···Ln···Al2	114.58(1)	117.47(3)	123.36(2)

to the orientation of the *t*Bu groups in the apertures between the two aluminate ligands, resulting in a staggered conformation (Figure 3 (bottom)). Nevertheless, the ^{1}H NMR spectra of **4** at ambient temperature show resonances of only two inequivalent *t*Bu groups due to ring rotation of the Cp^R rings about their pseudo C_5 axis.

Reactivity toward R_2AlCl: Mono(cyclopentadienyl) compounds $[Ln(AlMe_4)_2(Cp^R)]$ (**2–5**) feature a distinct pre-organized set of bridged, heterobimetallic Ln/Al moieties. Given the superb performance of Ln/Al heterobimetallic complexes such as $[Ln(AlMe_4)_3]$,[18,19] $[LnAl_3Me_8(O_2CC_6H_2iPr_3\text{-}2,4,6)_4]$, and $[Ln(AlMe_3)_n(OR)_3]$ (R = neopentyl, $C_6H_3R'_2$-2,6 (R′ = *t*Bu, *i*Pr)) as initiators for the *cis*-1,4 stereospecific polymerization of isoprene following activation with chloride donors such as Et_2AlCl or Ph_3CCl,[20] we investigated the catalytic potential of half-sandwich complexes $[Ln(AlMe_4)_2(Cp^R)]$. Accordingly, the initiating performance of $[Ln(AlMe_4)_2(Cp^R)]$ (**2–5**) in the polymerization of isoprene was examined in the presence of one, two, and three equivalents of diethylaluminum chloride Et_2AlCl as a "weakly cationizing" cocatalyst.

Contrary to the reported high activities of binary catalyst mixtures containing the above-mentioned non-cyclopentadienyl Ln/Al heterobimetallic complexes and Et_2AlCl, mixtures of **2–5** and Et_2AlCl did not provide active catalysts for the polymerization of isoprene. Treatment of $[Ln(AlMe_4)_2(C_5Me_5)]$ (**5**) (Ln = Y, Nd, La) with varying amounts of Me_2AlCl has recently been reported to yield mixed tetramethylaluminate/chloride compounds.[14] The extent of the $[AlMe_4] \rightarrow [Cl]$ exchange and the nuclearity of the resulting rare-earth metal complexes was found to be significantly affected by subtle changes in the rare-earth metal cation size. While alkyl/chloride interchange led to alkylated heterobimetallic half-sandwich $[La_6Al_4]$ and $[Nd_5Al]$ cluster compounds, chloro-bridged dimers $[Y_2Al_2]$ were obtained for the smaller yttrium metal center.

Addition of one equivalent of Me_2AlCl to solutions of half-sandwich complexes **2b**, **3b**, and **4d** in hexane yielded crystalline materials of the net composition $[Ln(AlMe_4)(Cl)(Cp^R)]$ (Ln = Y, Cp^R = [1,3-$(Me_3Si)_2C_5H_3$] (**6**); Ln = Y, Cp^R = ($C_5Me_4SiMe_3$) (**8**); and Ln = Nd, Cp^R = [1,2,4-$(Me_3C)_3C_5H_2$] (**9**)) in low to moderate yields (Scheme 2).[30] Molar ratios of Me_2AlCl/**2b** > 1.0 gave increasing amounts of an amorphous white solid material identified as $[\{YCl_2\{1,3\text{-}(Me_3Si)_2C_5H_3\}\}_n]$ (**7**) (Scheme 2).[31]

Complete $[AlMe_4] \rightarrow [Cl]$ exchange in **7** could be confirmed by ^{1}H and ^{13}C NMR spectroscopy in [D_6]benzene, which showed only the signals of the Cp^R ligand. Examination of the hexane-soluble fractions, however, revealed mixtures of unreacted $[Y(AlMe_4)_2\{1,3\text{-}(Me_3Si)_2C_5H_3\}]$ (**2b**) and

Table 3. Selected structural parameters [Å, °] for complexes **3b**, **4c**, **4d**, and **4e** (C_g = ring centroid).

	3b (Y)	**4c** (Sm)	**4d** (Nd)	**4e** (La)
Ln−C(Cp^R)	2.610(3)–2.695(3)	2.668(1)–2.748(1)	2.694(2)–2.768(2)	2.769(1)–2.838(1)
Ln−C_g	2.35	2.42	2.45	2.53
Ln−C1	2.530(3)	2.603(1)	2.626(2)	2.694(1)
Ln−C2	2.520(3)	2.618(1)	2.652(2)	2.716(1)
Ln−C5	2.680(3)	2.722(2)	2.748(2)	2.797(1)
Ln−C6	2.669(3)	2.672(2)	2.732(2)	2.790(2)
Al1−C1	2.063(3)	2.069(2)	2.067(2)	2.069(2)
Al1−C2	2.081(3)	2.070(2)	2.067(3)	2.061(2)
Al1−C3	1.983(4)	1.970(2)	1.960(3)	1.961(2)
Al1−C4	1.976(4)	1.969(2)	1.973(2)	1.975(2)
Al2−C5	2.054(3)	2.069(2)	2.059(2)	2.065(2)
Al2−C6	2.061(3)	2.075(2)	2.070(3)	2.067(2)
Al2−C7	1.982(4)	1.988(2)	1.994(3)	2.000(2)
Al2−C8	1.952(4)	1.954(2)	1.956(2)	1.959(2)
Ln···Al1	3.099(1)	3.1664(4)	3.1951(6)	3.2652(4)
Ln···Al2	2.929(1)	2.9855(4)	3.0035(6)	3.0494(4)
Ln···C7	3.297(4)	3.377(2)	3.326(3)	3.293(2)
C1-Ln-C2	83.16(11)	80.39(5)	79.40(7)	77.50(5)
C5-Ln-C6	76.31(10)	77.43(5)	76.30(7)	74.54(5)
Ln-C1-Al1	84.20(11)	84.51(5)	84.93(6)	85.49(4)
Ln-C2-Al1	84.09(11)	84.12(5)	84.27(8)	85.05(5)
Ln-C5-Al2	75.16(10)	75.73(4)	75.84(6)	76.03(4)
Ln-C6-Al2	75.32(10)	76.81(5)	76.03(7)	76.15(7)
C1-Al1-C2	108.0(1)	108.95(6)	109.26(8)	110.13(6)
C5-Al2-C6	106.8(1)	108.97(6)	110.12(9)	109.95(6)
C1-Al1-C3	108.2(2)	105.32(8)	104.2(1)	104.35(7)
C1-Al1-C4	109.2(2)	110.97(8)	111.4(1)	110.84(8)
C5-Al2-C7	107.8(2)	104.96(8)	105.1(1)	104.56(7)
C5-Al2-C8	109.9(2)	110.36(7)	110.2(1)	111.19(8)
Al1···Ln···Al2	110.25(3)	113.45(1)	115.04(2)	115.44(1)

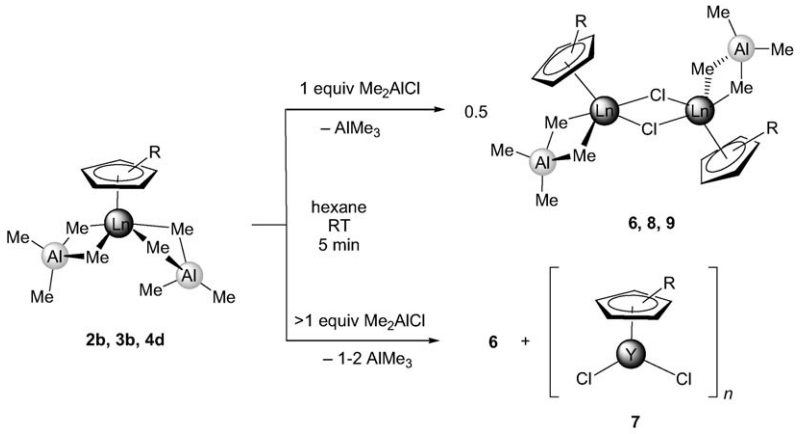

Scheme 2. Synthesis of $[Ln(AlMe_4)(\mu\text{-}Cl)(Cp^R)]_2$ (Ln = Y, $Cp^R = [1,3\text{-}(Me_3Si)_2C_5H_3]$ (**6**); Ln = Y, $Cp^R = (C_5Me_4SiMe_3)$ (**8**); Ln = Nd, $Cp^R = [1,2,4\text{-}(Me_3C)_3C_5H_2]$ (**9**)) and $[YCl_2(Cp^R)]_n$ ($Cp^R = [1,3\text{-}(Me_3Si)_2C_5H_3]$, $n > 1$) (**7**).

$[\{Y(AlMe_4)(\mu\text{-}Cl)\{1,3\text{-}(Me_3Si)_2C_5H_3\}\}_2]$ (**6**), irrespective of the amount of Me_2AlCl used.

X-ray structure analyses of compounds **8** and **9** revealed dimeric complexes $[\{Y(AlMe_4)(\mu\text{-}Cl)(C_5Me_4SiMe_3)\}_2]$ (Figure 4, top) and $[\{Nd(AlMe_4)(\mu\text{-}Cl)\{1,2,4\text{-}(Me_3C)_3C_5H_2\}\}_2]$ (Figure 4, bottom) with formally heptacoordinate lanthanide metal centers and a rare combination of homometal-bridging chloride ligands and η^2-coordinated aluminate ligands. The average Y−C(μ-Me) bond length of 2.551 Å in **8** appears slightly elongated compared to that of the η^2-coordinated aluminate ligand of the respective precursor compound (av. 2.525 Å (**3b**)) and is significantly longer than similar bonds in homoleptic $[Y(AlMe_4)_3]$ (av. 2.508 Å (**1b**), Table 4).[32] The solid-state structure of complex **9** revealed a slightly bent aluminate ligand (interplanar angle NdC1C2-Al1C1C2 26.1(14)°, Nd···C3 4.075(3) Å) and an average Nd−C(μ-Me) bond distance of 2.637 Å (Table 4). For comparison, the Nd−C(μ-Me) aluminate bond lengths range from 2.639 Å (η^2) to 2.740 Å (bent η^2) in precursor compound **4d** and average 2.592 Å in homoleptic $[Nd(AlMe_4)_3]$ (**1d**).[32] The Ln−Cl bond distances (av. 2.693 Å (**8**); av. 2.794 Å (**9**)) are comparable to the corresponding bond lengths of the bridging chloro ligands in dimeric $[\{Y(AlMe_4)(\mu\text{-}Cl)(C_5Me_5)\}_2]$ (av. 2.6752 Å) and the $[\mu_2\text{-}Cl]$ bridges in the pentanuclear neodymium cluster $[Nd_5(\mu_4\text{-}Cl)(\mu_3\text{-}Cl)_2(\mu_2\text{-}Cl)_6(C_5Me_5)_5\{(\mu\text{-}Me)_3\text{-}AlMe\}]$ (2.775 Å).[14]

Mixed tetramethylaluminate/chloride complexes **6**, **8**, and **9** are sparingly soluble in hydrocarbon solvents but readily dissolve in aromatic solvents. The ^{1}H NMR spectra of diamagnetic **6** and **8** in [D_6]benzene feature sets of signals due to the respective Cp^R ligands and the $[AlMe_4]$ moiety, which are slightly shifted to lower field compared with those of the precursor compounds **2b** and **3b** (Table 1), albeit with the same two-bond ^{1}H-^{89}Y scalar couplings of $^2J_{YH} = 2.4$ Hz (**6**) and $^2J_{YH} = 2.0$ Hz (**7**). The observed downfield shift is in accordance with a comparatively weakened coordination of the $[AlMe_4]$ ligands to the rare-earth metal center and is somewhat contrary to an anticipated cationization of complexes $[Ln(AlMe_4)_2(Cp^R)]$ by dialkylaluminum chlorides (cationization of $[Ln(AlMe_4)_2(Cp^R)]$ by borate or borane activators results in upfield shifts in accordance with a stronger ligand

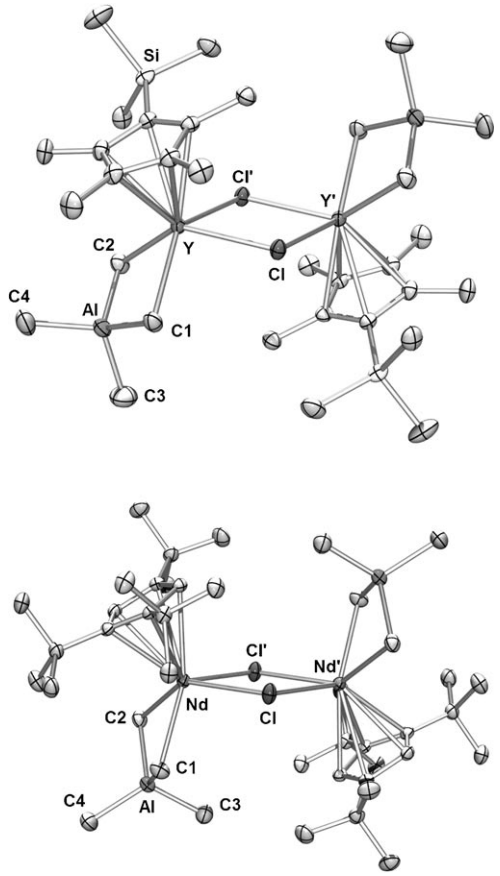

Figure 4. Molecular structures of **8** (top) and **9** (bottom) (atomic displacement parameters are set at the 50% level). Hydrogen atoms have been omitted for clarity. Symmetry code for (′) depicts $(-x+1, -y, -z+1)$ for **8** and $(-x+1, -y+1, -z+2)$ for **9**.

Table 4. Selected structural parameters [Å, °] for complexes **8** and **9** (C_g = ring centroid). Symmetry code for (′) is $(-x+1, -y, -z+1)$ for **8** and $(-x+1, -y+1, -z+2)$ for **9**).

	8 (Y)	**9** (Nd)
Ln−C(Cp^R)	2.566(1)–2.645(1)	2.690(2)–2.762(2)
Ln−C_g	2.30	2.44
Ln−C1	2.558(2)	2.620(2)
Ln−C2	2.543(2)	2.653(2)
Ln−Cl1/Cl1′	2.6803(4)/2.7061(4)	2.7807(6)/2.8077(6)
Al1−C1	2.074(2)	2.078(2)
Al1−C2	2.073(2)	2.067(2)
Al1−C3	1.968(2)	1.970(3)
Al1−C4	1.969(2)	1.967(3)
Ln···Al1	3.0992(5)	3.1646(7)
C1-Ln-C2	82.93(6)	79.23(7)
Ln-C1-Al1	83.30(6)	83.84(8)
Ln-C2-Al1	83.67(2)	83.22(8)
Ln-Cl1-Ln′	102.12(1)	106.27(2)
C1-Al1-C2	109.06(7)	108.42(10)
C1-Al1-C3	109.00(9)	105.52(11)
C1-Al1-C4	105.46(9)	107.55(12)

coordination to the electron-deficient rare-earth metal cation, Table 1). Significant paramagnetic shifts and broadening effects were observed in the ^{1}H NMR spectrum of the neodymium complex **9**.

Contrary to the cluster formation observed for reactions of $[Ln(AlMe_4)_2(C_5Me_5)]$ (**5**) (Ln = Nd, La) with Me_2AlCl,[14] well-defined dimeric compounds $[\{Ln(AlMe_4)(\mu\text{-}Cl)(Cp^R)\}_2]$ were exclusively found for $Cp^R = [1,3\text{-}(Me_3Si)_2C_5H_3]$, $[C_5Me_4SiMe_3]$, and $[1,2,4\text{-}(Me_3C)_3C_5H_2]$, even for the large neodymium metal center in **9**. Such dinuclear compounds are formed in mixtures of **2**–**4** with Et_2AlCl as sterically and electronically saturated systems without catalytic activity toward isoprene polymerization.

Polymerization of isoprene: We recently reported new initiators for the controlled polymerization of isoprene based on half-sandwich complexes $[Ln(AlMe_4)_2(C_5Me_5)]$ (**5**) and fluorinated borate and borane reagents as cationizing agents.[22] Remarkably, such mixtures yielded polyisoprene with a very high *trans*-1,4 content. Catalyst activities and selectivities showed a strong dependence on the size of the rare-earth metal cation and the nature of the boron cocatalyst. Half-sandwich complexes **2**–**4** were therefore employed as precatalysts in the polymerization of isoprene. The polymerization results are summarized in Table 5, along with data for catalysts based on $[Ln(AlMe_4)_2(C_5Me_5)]$ (**5**) taken from a previous study, which was performed under similar conditions (see Experimental Section).[22]

Effect of the metal center: For a systematic investigation of the effect of the rare-earth metal on catalytic activities and catalyst selectivity, yttrium and lanthanum were selected representing one of the smaller and the largest rare-earth metal center for half-sandwich complexes **2** (Table 5, entries 1–6) and **3** (Table 5, entries 7–12). Due to the unavailability of complexes **4** for the smaller rare-earth metal centers, the neodymium and lanthanum derivatives **4d** and **4e** were chosen (Table 5, entries 13–18). All precatalysts under investigation showed extremely high activities upon cationization with $[Ph_3C][B(C_6F_5)_4]$ (**A**) or $[PhNMe_2H][B(C_6F_5)_4]$ (**B**) as activators. No significant effect of the size of the metal cation on the catalytic activity was observed.

The activities obtained for catalyst systems activated by $B(C_6F_5)_3$ (**C**) were comparatively low, and were also only marginally affected by the Ln^{III} size. While the effect of the metal on the catalytic activity is less pronounced, the choice of metal center significantly affects the selectivity of the catalyst. In a previous study, we showed that the lanthanum half-sandwich complexes $[La(AlMe_4)_2(C_5Me_5)]$ (**5e**) greatly outperform their corresponding yttrium and neodymium congeners **5b** and **5d**, respectively (Table 5, runs 19–27).[22] Similar effects have now been observed for complexes **2**, **3**, and **4**. The *trans*-selectivity increases remarkably with increasing size of the rare-earth metal cation (La ≫ Y: Table 5, runs 4–6, 10–12, 16–18, 25–27).

Effect of the substituted cyclopentadienyl ancillary ligand: Quantitative polymer formation was observed in all experiments, irrespective of the substitution pattern on the cyclopentadienyl ancillary ligand (Cp^R). No effect of the steric bulk of the ligands on catalytic activity could be discerned.

Table 5. Effect of Ln size, Cp substituent, and cocatalyst on the polymerization of isoprene.

Entry[a]	Precatalyst	Cocatalyst[b]	Yield	Structure[c]			M_n[d]	M_w/M_n	Efficiency[e]
			[%]	*trans*-1,4-	*cis*-1,4-	3,4-	($\times 10^5$)		[%]
1	$[Y(AlMe_4)_2\{1,3\text{-}(Me_3Si)_2C_5H_3\}]$ (**2b**)	A	>99	9.0	60.0	31.0	1.9	2.18	0.35
2	$[Y(AlMe_4)_2\{1,3\text{-}(Me_3Si)_2C_5H_3\}]$ (**2b**)	B	>99	4.0	63.0	33.0	1.2	1.77	0.57
3	$[Y(AlMe_4)_2\{1,3\text{-}(Me_3Si)_2C_5H_3\}]$ (**2b**)	C	>99	40.0	52.0	8.0	2.7	1.74	2.57
4	$[La(AlMe_4)_2\{1,3\text{-}(Me_3Si)_2C_5H_3\}]$ (**2e**)	A	>99	80.3	14.5	5.2	0.6	1.28	1.12
5	$[La(AlMe_4)_2\{1,3\text{-}(Me_3Si)_2C_5H_3\}]$ (**2e**)	B	>99	79.4	15.3	5.3	0.6	1.22	1.15
6	$[La(AlMe_4)_2\{1,3\text{-}(Me_3Si)_2C_5H_3\}]$ (**2e**)	C	>99	89.3	–	10.7	3.3	1.52	0.21
7	$[Y(AlMe_4)_2(C_5Me_4SiMe_3)]$ (**3b**)	A	>99	26.4	38.1	35.5	0.1	20.41	5.59
8	$[Y(AlMe_4)_2(C_5Me_4SiMe_3)]$ (**3b**)	B	>99	34.6	38.3	27.1	0.3	1.74	2.11
9	$[Y(AlMe_4)_2(C_5Me_4SiMe_3)]$ (**3b**)	C	>99	80.8	3.4	15.8	0.5	1.73	1.42
10	$[La(AlMe_4)_2(C_5Me_4SiMe_3)]$ (**3e**)	A	>99	81.4	3.4	15.2	0.9	1.45	0.79
11	$[La(AlMe_4)_2(C_5Me_4SiMe_3)]$ (**3e**)	B	>99	87.7	10.5	1.8	0.6	1.20	1.20
12	$[La(AlMe_4)_2(C_5Me_4SiMe_3)]$ (**3e**)	C	>99	95.6	2.2	2.2	2.0	1.26	0.34
13	$[Nd(AlMe_4)_2\{1,2,4\text{-}(Me_3C)_3C_5H_2\}]$ (**4d**)	A	>99	21.2	45.5	33.5	0.8	1.67	0.83
14	$[Nd(AlMe_4)_2\{1,2,4\text{-}(Me_3C)_3C_5H_2\}]$ (**4d**)	B	>99	19.0	53.0	28.0	0.9	1.25	0.80
15	$[Nd(AlMe_4)_2\{1,2,4\text{-}(Me_3C)_3C_5H_2\}]$ (**4d**)	C	>99	56.0	31.0	13.0	0.5	1.50	1.37
16	$[La(AlMe_4)_2\{1,2,4\text{-}(Me_3C)_3C_5H_2\}]$ (**4e**)	A	>99	60.0	20.0	20.0	0.8	1.41	0.82
17	$[La(AlMe_4)_2\{1,2,4\text{-}(Me_3C)_3C_5H_2\}]$ (**4e**)	B	>99	50.0	30.0	20.0	0.8	1.22	0.91
18	$[La(AlMe_4)_2\{1,2,4\text{-}(Me_3C)_3C_5H_2\}]$ (**4e**)	C	>99	90.0	6.0	4.0	1.1	1.41	0.60
19	$[Y(AlMe_4)_2(C_5Me_5)]$ (**5b**)	A	>99	20.6	60.5	18.9	0.2	8.95	3.98
20	$[Y(AlMe_4)_2(C_5Me_5)]$ (**5b**)	B	>99	28.7	43.5	27.8	0.6	1.59	1.06
21	$[Y(AlMe_4)_2(C_5Me_5)]$ (**5b**)	C	>99	93.6	1.9	4.5	0.9	1.78	0.82
22	$[Nd(AlMe_4)_2(C_5Me_5)]$ (**5d**)	A	>99	69.7	14.0	16.3	0.3	2.87	2.11
23	$[Nd(AlMe_4)_2(C_5Me_5)]$ (**5d**)	B	>99	79.9	6.9	13.2	0.4	1.16	1.73
24	$[Nd(AlMe_4)_2(C_5Me_5)]$ (**5d**)	C	>99	92.4	3.8	3.8	1.3	1.35	0.52
25	$[La(AlMe_4)_2(C_5Me_5)]$ (**5e**)	A	>99	87.0	3.5	9.5	0.7	1.28	1.98
26	$[La(AlMe_4)_2(C_5Me_5)]$ (**5e**)	B	>99	79.5	3.4	17.1	0.6	1.22	1.08
27	$[La(AlMe_4)_2(C_5Me_5)]$ (**5e**)	C	>99	99.5	–	0.5	2.4	1.18	0.28

[a] Conditions: 0.02 mmol precatalyst, [Ln]/[cocat] = 1:1, 8 mL toluene, 20 mmol isoprene, 24 h, 40 °C. [b] Cocatalyst: **A** = $[Ph_3C][B(C_6F_5)_4]$, **B** = $[PhNMe_2H][B(C_6F_5)_4]$, **C** = $B(C_6F_5)_3$; the catalyst was preformed for 20 min at 40 °C. [c] Determined by ^1H and ^{13}C NMR spectroscopy in $CDCl_3$. [d] Determined by means of size-exclusion chromatography (SEC) against polystyrene standards. [e] Initiation efficiency = M_n(calculated)/M_n(measured).

Little correlation between the degree of steric shielding and the observed stereospecificities was noted. Rather, the stereospecificity seems to be affected by the electronic properties of the Cp^R ligand and its propensity to undergo degradation reactions ($[C_5Me_5] \ll [C_5Me_4SiMe_3] < [1,2,4\text{-}(Me_3C)_3C_5H_2] \ll [1,3\text{-}(Me_3Si)_2C_5H_3]$). These findings are in good agreement with the stabilities of cationic species generated in mixtures $[Ln(AlMe_4)_2(Cp^R)]$/borate or $[Ln(AlMe_4)_2(Cp^R)]/B(C_6F_5)_3$ as monitored by ^1H NMR experiments. The cation stability significantly decreases in the series $[C_5Me_5] \gg [C_5Me_4SiMe_3] > [1,2,4\text{-}(Me_3C)_3C_5H_2] \gg [1,3\text{-}(Me_3Si)_2C_5H_3]$, which is manifested in extensive ancillary ligand degradation for cationic complexes containing the latter two substituted cyclopentadienyl ligands.

Effect of the boron cocatalyst: As previously reported for $[Ln(AlMe_4)_2(C_5Me_5)]$ (**5**),[22] the reactions of $[Ln(AlMe_4)_2(Cp^R)]$ (**2**–**4**) with one equivalent of $[Ph_3C][B(C_6F_5)_4]$ (**A**) or $[PhNMe_2H][B(C_6F_5)_4]$ (**B**) yield tight ion pairs $[Ln(AlMe_4)(Cp^R)][B(C_6F_5)_4]$ (**9**). ^1H NMR spectroscopy clearly indicated instant disappearance of the signals of **2**–**4**. Upon reaction with $[Ph_3C][B(C_6F_5)_4]$, quantitative formation of Ph_3CMe and one equivalent $AlMe_3$ was observed, while the reaction with $[PhNMe_2H][B(C_6F_5)_4]$ was accompanied by quantitative formation of $PhNMe_2$ and one equivalent each of $AlMe_3$ and CH_4. New signals due to the respective Cp^R ligands appeared, with slight upfield shifts in accordance with stronger coordination to the highly electron-deficient lanthanide cation. The use of $[Ph_3C][B(C_6F_5)_4]$ and $[PhNMe_2H][B(C_6F_5)_4]$ as activators for $[(Cp^R)Ln(AlMe_4)_2]$ led to extremely high activity in the polymerization reactions. The activities of 68 $kg\,mol^{-1}\,h^{-1}$ are twofold higher than those mentioned in the literature for similar *trans*-specific polymerizations.[33–35] However, the *trans*-1,4 content in the resulting polyisoprene did not exceed 88%, even for catalyst systems based on the large lanthanum metal center (Table 5, runs 4/5, 10/11, 16/17, 25/26). In accordance with a different activation mechanism, the use of $B(C_6F_5)_3$ (**C**) as an activator for complexes $[Ln(AlMe_4)_2(Cp^R)]$ resulted in the formation of a catalytically active species with a markedly different performance. Active species formed in mixtures of $[Ln(AlMe_4)_2(Cp^R)]/B(C_6F_5)_3$[36] polymerized isoprene with comparatively low activities but with a high to very high *trans*-1,4 content and very narrow molecular weight distributions (Table 5). The highest *trans*-1,4 selectivities were observed with the large rare-earth metal center lanthanum, especially for precatalysts $[La(AlMe_4)_2(C_5Me_4SiMe_3)]$ (**3e**; *trans*-1,4 content: 95.6%, $M_w/M_n = 1.26$) and $[La(AlMe_4)_2(C_5Me_5)]$ (**5e**; *trans*-1,4 content: 99.5%, $M_w/M_n = 1.18$) (Table 5, runs 12 and 27; Figure 5).

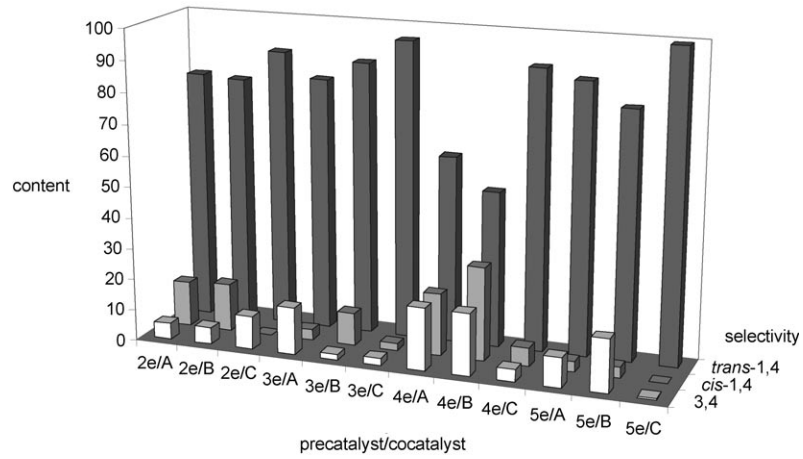

Figure 5. Representation of the *trans*-1,4-, *cis*-1,4-, and 3,4-contents of the polyisoprenes obtained from $[La(AlMe_4)_2(Cp^R)]$ (**2e**, **3e**, **4e**, and **5e**) and cocatalysts **A**, **B**, and **C**.

Conclusion

The "aluminate route" offers a viable synthesis protocol for generating a series of donor-solvent-free half-sandwich complexes $[Ln(AlMe_4)_2(Cp^R)]$ bearing cyclopentadienyl ligands with various stereoelectronic properties. X-ray structure analyses covering $[Ln(AlMe_4)_2(Cp^R)]$ compounds with differently substituted cyclopentadienyl ligands, as well as a wide size range of Ln^{III} cations, have revealed similar structural motifs irrespective of the Cp^R ancillary ligand and the size of the rare-earth metal cation involved. All of the solid-state structures feature one η^2-coordinating planar $[AlMe_4]$ ligand, whereas the second such ligand shows a bent η^2-coordination mode, allowing for an additional short Ln···(μ-Me) contact. These half-sandwich bis(tetramethylaluminate) complexes showed no catalytic activity in the polymerization of isoprene upon addition of one, two, or three equivalents of dialkylaluminum chloride reagents. Instead, mixtures of $[Ln(AlMe_4)_2(Cp^R)]/Me_2AlCl$ yielded discrete dimeric mixed tetramethylaluminate/chloride complexes $[\{Ln(AlMe_4)(\mu\text{-}Cl)(Cp^R)\}_2]$ and higher agglomerated fully exchanged derivatives $[\{Ln(\mu\text{-}Cl)_2(Cp^R)\}_n]$. However, catalytically active systems were obtained when fluorinated borate and borane reagents were applied as cocatalysts. Systematic investigations of the effects of metal cation size, the substituents on the cyclopentadiene ligand, and cocatalyst interactions (borate vs. borane) have revealed: a) good (for systems activated with $B(C_6F_5)_3$) to excellent catalytic activities for $[Ln(AlMe_4)_2(Cp^R)]$ activated by borate cocatalysts $[Ph_3C][B(C_6F_5)_4]$ or $[PhNMe_2H][B(C_6F_5)_4]$, b) increased *trans*-1,4 selectivity with increasing size of the rare-earth metal cation (Y < Nd ≪ La), c) increased *trans*-1,4 selectivity with enhanced chemical "innocence" and stability of the Cp^R ligand ($[1,3\text{-}(Me_3Si)_2C_5H_3]$ ≪ $[1,2,4\text{-}(Me_3C)_3C_5H_2]$ < $[C_5Me_4SiMe_3]$ ≪ $[C_5Me_5]$). The highest stereoselectivities were observed for the precatalyst/cocatalyst systems $[La(AlMe_4)_2(C_5Me_4SiMe_3)]/B(C_6F_5)_3$ (*trans*-1,4 content: 95.6%, $M_w/M_n = 1.26$) and $[La(AlMe_4)_2(C_5Me_5)]/B(C_6F_5)_3$ (*trans*-1,4 content: 99.5%, $M_w/M_n = 1.18$).

Experimental Section

General remarks: All operations were performed with rigorous exclusion of air and water, using standard Schlenk, high-vacuum, and glovebox techniques (MBraun MBLab; <1 ppm O_2, <1 ppm H_2O). Hexane and toluene were purified by using Grubbs columns (MBraun SPS, solvent purification system) and were stored in a glovebox. $[D_6]$Benzene was obtained from Aldrich, degassed, dried over Na for 24 h, and filtered. $C_5HMe_4SiMe_3$, $AlMe_3$, and Me_2AlCl were purchased from Aldrich and were used as received. $[Ph_3C][B(C_6F_5)_4]$, $[PhNMe_2H][B(C_6F_5)_4]$, and $[B(C_6F_5)_3]$ were purchased from Boulder Scientific Company and were used without further purification. Homoleptic $[Ln(AlMe_4)_3]$ (**1**) (Ln = Lu, Y, Sm, Nd, La),[9] $[1,3\text{-}(Me_3Si)_2C_5H_4]$,[24] $[1,2,4\text{-}(Me_3C)_3C_5H_3]$,[26] and $[Ln(AlMe_4)_2(C_5Me_5)]$ (**5**) (Ln = Y, Nd, La)[8] were synthesized according to literature methods. Isoprene was obtained from Aldrich, dried several times over activated 3 Å molecular sieves, and distilled prior to use. The NMR spectra of air- and moisture-sensitive compounds were recorded at 25 °C on a Bruker BIOSPIN AV500 (5 mm BBO, ^1H: 500.13 Hz; ^{13}C: 125.77 MHz) or a Bruker BIOSPIN AV600 (5 mm cryo probe, ^1H: 600.13 MHz; ^{13}C: 150.91 MHz) with samples in J. Young valve NMR tubes. ^1H and ^{13}C shifts are referenced to internal solvent resonances and are reported in parts per million relative to TMS. IR spectra were recorded on a NICOLET Impact 410 FTIR spectrometer from samples in Nujol mulls sandwiched between CsI plates. Elemental analyses were performed on an Elementar Vario EL III. The molar masses (M_w/M_n) of the polymers were determined by size-exclusion chromatography (SEC). Sample solutions (1.0 mg polymer per mL THF) were filtered through a 0.2 μm syringe filter prior to injection. SEC was operated with a pump supplied by Waters (Waters 510), employing Ultrastyragel® columns with pore sizes of 500, 1000, 10000, and 100000 Å. Signals were detected by means of a differential refractometer (Waters 410) and calibrated against polystyrene standards ($M_w/M_n < 1.15$). The flow rate was 1.0 mL min^{-1}. The microstructure of the polyisoprenes was examined by means of ^1H and ^{13}C NMR experiments on the AV500 spectrometer at ambient temperature, using [D]chloroform as solvent and TMS as internal standard.

General procedure for the preparation of $[Ln(AlMe_4)_2\{1,3\text{-}(Me_3Si)_2C_5H_3\}]$ (2) and $[Ln(AlMe_4)_2(C_5Me_4SiMe_3)]$ (3): In a glovebox, $[Ln(AlMe_4)_3]$ (**1**) was dissolved in hexane (2 mL), and then a solution of either $[1,3\text{-}(Me_3Si)_2C_5H_4]$ (1 equiv) or $(C_5HMe_4SiMe_3)$ (1 equiv) in hexane (2 mL) was added to the alkylaluminate solution under vigorous stirring. Upon the addition, instant gas formation was observed. After the reaction mixture had been stirred for a further 5 h at ambient temperature, the solvent was removed in vacuo to give **2** or **3** as crystalline solids. Crystallization from a solution in hexane at −35 °C gave high yields of single crystals of **2** or **3** suitable for X-ray diffraction analysis.

$[Lu(AlMe_4)_2\{1,3\text{-}(Me_3Si)_2C_5H_3\}]$ (2a): Following the procedure described above, $[Lu(AlMe_4)_3]$ (**1a**) (227 mg, 0.52 mmol) and $[1,3\text{-}(Me_3Si)_2C_5H_4]$ (109 mg, 0.52 mmol) yielded **2a** (145 mg, 0.26 mmol, 50%) as colorless crystals. ^1H NMR (500 MHz, $[D_6]$benzene, 25 °C): $\delta = 6.53$ (d, $^3J = 1.5$ Hz, 1H; CpH), 6.53 (s, 1H; CpH), 6.52 (d, $^3J = 1.5$ Hz, 1H; CpH), 0.17 (s, 18H; $Si(CH_3)_3$), −0.14 ppm (s, 24H; $Al(CH_3)_4$); ^{13}C NMR (126 MHz, $[D_6]$benzene, 25 °C): $\delta = 125.7$, 118.4, 114.8 (Cp), 1.5 (br s; $Al(CH_3)_4$), 0.2 ppm ($Si(CH_3)_3$); IR (Nujol): $\tilde{\nu} = 1463$ (vs, Nujol), 1375 (vs, Nujol), 1318 (w), 1303 (w), 1251 (s), 1204 (m), 1194 (m), 1080 (s), 925 (s), 837 (s), 759 (m), 723 (s), 692 (m), 640 (w), 578 (m), 567 cm^{-1} (w); elemental analysis calcd (%) for $C_{19}H_{45}Al_2Si_2Lu$ (558.67): C 40.85, H 8.12; found: C 41.03, H 7.94.

[Y(AlMe$_4$)$_2${1,3-(Me$_3$Si)$_2$C$_5$H$_3$}] (2b): Following the procedure described above, [Y(AlMe$_4$)$_3$] (**1b**) (350 mg, 1.00 mmol) and [1,3-(Me$_3$Si)$_2$C$_5$H$_4$] (211 mg, 1.00 mmol) yielded **2b** (463 mg, 0.98 mmol, 98%) as colorless crystals. ^{1}H NMR (600 MHz, [D$_6$]benzene, 25°C): δ = 6.62 (d, ^3J = 1.5 Hz, 1H; CpH), 6.62 (s, 1H; CpH), 6.61 (d, ^3J = 1.5 Hz, 1H; CpH), 0.17 (s, 18H; Si(CH$_3$)$_3$), −0.29 ppm (d, $^2J_{YH}$ = 2.4 Hz, 24H; Al(CH$_3$)$_4$); ^{13}C{^{1}H} NMR (151 MHz, [D$_6$]benzene, 25°C): δ = 129.4, 129.3, 126.9 (Cp), 0.2 (Si(CH$_3$)$_3$), 0.0 ppm (brs; Al(CH$_3$)$_4$); IR (Nujol): $\tilde{\nu}$ = 1458 (vs, Nujol), 1375 (vs, Nujol), 1328 (w), 1251 (s), 1204 (m), 1194 (m), 1080 (s), 925 (s), 837 (s), 759 (m), 723 (s), 697 (s), 655 (m), 578 (m), 567 cm^{-1} (w); elemental analysis calcd (%) for C$_{19}$H$_{45}$Al$_2$Si$_2$Y (472.61): C 48.29, H 9.60; found: C 48.35, H 9.67.

[Sm(AlMe$_4$)$_2${1,3-(Me$_3$Si)$_2$C$_5$H$_3$}] (2c): Following the procedure described above, [Sm(AlMe$_4$)$_3$] (**1c**) (299 mg, 0.73 mmol) and [1,3-(Me$_3$Si)$_2$C$_5$H$_4$] (153 mg, 0.73 mmol) yielded **2c** (355 mg, 0.66 mmol, 91%) as dark-red crystals. ^{1}H NMR (500 MHz, [D$_6$]benzene, 25°C): δ = −0.76 (brs, 2H; CpH), −0.96 (s, 18H; Si(CH$_3$)$_3$), −1.40 (s, 1H; CpH), −2.81 ppm (s, 24H; Al(CH$_3$)$_4$); ^{13}C NMR (126 MHz, [D$_6$]benzene, 25°C): δ = 125.6, 120.8, 115.1 (Cp), −1.6 (Si(CH$_3$)$_3$), −20.1 ppm (brs; Al(CH$_3$)$_4$); IR (Nujol): $\tilde{\nu}$ = 1458 (vs, Nujol), 1375 (vs, Nujol), 1318 (w), 1256 (s), 1214 (m), 1183 (m), 1090 (s), 925 (s), 837 (s), 759 (m), 723 (s), 686 (s), 645 (m), 629 (m), 583 (m), 541 (w), 516 cm^{-1} (w); elemental analysis calcd (%) for C$_{19}$H$_{45}$Al$_2$Si$_2$Sm (534.06): C 42.73, H 8.49; found: C 42.61, H 8.54.

[Nd(AlMe$_4$)$_2${1,3-(Me$_3$Si)$_2$C$_5$H$_3$}] (2d): Following the procedure described above, [Nd(AlMe$_4$)$_3$] (**1d**) (252 mg, 0.62 mmol) and [1,3-(Me$_3$Si)$_2$C$_5$H$_4$] (131 mg, 0.62 mmol) yielded **2d** (295 mg, 0.56 mmol, 90%) as blue crystals. ^{1}H NMR (500 MHz, [D$_6$]benzene, 25°C): δ = 6.78 (brs, 24H; Al(CH$_3$)$_4$), 5.40 (brs, 2H; CpH), 4.98 (brs, 1H; CpH), −3.94 ppm (s, 18H; Si(CH$_3$)$_3$); ^{13}C NMR (126 MHz, [D$_6$]benzene, 25°C): δ = 245.6 (brs; Al(CH$_3$)$_4$), 215.1, 213.0, 128.9 (Cp), 4.49 ppm (Si(CH$_3$)$_3$); IR (Nujol): $\tilde{\nu}$ = 1463 (vs, Nujol), 1379 (vs, Nujol), 1317 (w), 1254 (s), 1219 (m), 1179 (m), 1081 (s), 917 (s), 837 (s), 757 (m), 726 (s), 686 (s), 642 (m), 584 (m), 544 (w), 513 cm^{-1} (w); elemental analysis calcd (%) for C$_{19}$H$_{45}$Al$_2$Si$_2$Nd (527.94): C 43.23, H 8.59; found: C 43.17, H 8.49.

[La(AlMe$_4$)$_2${1,3-(Me$_3$Si)$_2$C$_5$H$_3$}] (2e): Following the procedure described above, [La(AlMe$_4$)$_3$] (**1e**) (256 mg, 0.64 mmol) and [1,3-(Me$_3$Si)$_2$C$_5$H$_4$] (135 mg, 0.64 mmol) yielded **2e** (328 mg, 0.63 mmol, 98%) as colorless crystals. ^{1}H NMR (500 MHz, [D$_6$]benzene, 25°C): δ = 6.78 (d, ^3J = 1.5 Hz, 1H; CpH), 6.77 (s, 1H; CpH), 6.77 (d, ^3J = 1.5 Hz, 1H; CpH), 0.17 (s, 18H; Si(CH$_3$)$_3$), −0.23 ppm (s, 24H; Al(CH$_3$)$_4$); ^{13}C{^{1}H} NMR (126 MHz, [D$_6$]benzene, 25°C): δ = 133.1, 131.9, 129.1 (Cp), 2.3 (brs; Al(CH$_3$)$_4$), 0.3 ppm (Si(CH$_3$)$_3$); IR (Nujol): $\tilde{\nu}$ = 1459 (vs, Nujol), 1374 (vs, Nujol), 1321 (w), 1254 (s), 1214 (m), 1192 (m), 1077 (s), 917 (s), 837 (s), 757 (m), 722 (s), 682 (s), 638 (m), 589 (m), 536 (w), 513 cm^{-1} (w); elemental analysis calcd (%) for C$_{19}$H$_{45}$Al$_2$Si$_2$La (522.61): C 43.67, H 8.68; found: C 43.94, H 8.46.

[Lu(AlMe$_4$)$_2$(C$_5$Me$_4$SiMe$_3$)] (3a): Following the procedure described above, [Lu(AlMe$_4$)$_3$] (**1a**) (214 mg, 0.49 mmol) and [C$_5$HMe$_4$SiMe$_3$] (95 mg, 0.49 mmol) yielded **3a** (255 mg, 0.47 mmol, 95%) as colorless crystals. ^{1}H NMR (500 MHz, [D$_6$]benzene, 25°C): δ = 1.99 (s, 6H; CH$_3$), 1.75 (s, 6H; CH$_3$), 0.22 (s, 9H; Si(CH$_3$)$_3$), −0.14 ppm (s, 24H; Al(CH$_3$)$_4$); ^{13}C{^{1}H} NMR (126 MHz, [D$_6$]benzene, 25°C): δ = 130.1, 126.5, 117.5 (Cp), 14.8 (CH$_3$), 12.0 (CH$_3$), 2.2 (Si(CH$_3$)$_3$), 1.7 ppm (brs, Al(CH$_3$)$_4$); IR (Nujol): $\tilde{\nu}$ = 1461 (vs, Nujol), 1378 (vs, Nujol), 1323 (m), 1256 (s), 1234 (w), 1212 (w), 1019 (w), 842 (s), 765 (m), 726 (s), 704 (s), 638 (w), 583 (m), 555 cm^{-1} (w); elemental analysis calcd (%) for C$_{20}$H$_{45}$Al$_2$SiLu (542.60): C 44.27, H 8.36; found: C 43.87, H 8.26.

[Y(AlMe$_4$)$_2$(C$_5$Me$_4$SiMe$_3$)] (3b): Following the procedure described above, [Y(AlMe$_4$)$_3$] (**1b**) (217 mg, 0.62 mmol) and [C$_5$HMe$_4$SiMe$_3$] (121 mg, 0.62 mmol) yielded **3b** (277 mg, 0.61 mmol, 98%) as colorless crystals. ^{1}H NMR (500 MHz, [D$_6$]benzene, 25°C): δ = 2.00 (s, 6H; CH$_3$), 1.75 (s, 6H; CH$_3$), 0.23 (s, 9H; Si(CH$_3$)$_3$), −0.31 ppm (d, $^2J_{YH}$ = 2.0 Hz, 24H; Al(CH$_3$)$_4$); ^{13}C{^{1}H} NMR (126 MHz, [D$_6$]benzene, 25°C): δ = 131.3, 128.3, 118.8 (Cp), 14.8 (CH$_3$), 11.9 (CH$_3$), 2.0 (Si(CH$_3$)$_3$), 0.1 ppm (brs; Al(CH$_3$)$_4$); IR (Nujol): $\tilde{\nu}$ = 1465 (vs, Nujol), 1375 (vs, Nujol), 1328 (m), 1254 (s), 1233 (w), 1222 (w), 1196 (m), 1133 (w), 1085 (w), 1022 (w), 974 (w), 837 (s), 764 (m), 716 (s), 637 (w), 595 (m), 516 cm^{-1} (w); elemental analysis calcd (%) for C$_{20}$H$_{45}$Al$_2$SiY (456.53): C 52.62, H 9.94; found: C 52.93, H 9.67.

[Sm(AlMe$_4$)$_2$(C$_5$Me$_4$SiMe$_3$)] (3c): Following the procedure described above, [Sm(AlMe$_4$)$_3$] (**1c**) (305 mg, 0.74 mmol) and [C$_5$HMe$_4$SiMe$_3$] (144 mg, 0.74 mmol) yielded **3c** (357 mg, 0.69 mmol, 93%) as dark-red crystals. ^{1}H NMR (500 MHz, [D$_6$]benzene, 25°C): δ = 2.69 (s, 6H; CH$_3$), −0.15 (s, 6H; CH$_3$), −0.66 (s, 9H; Si(CH$_3$)$_3$), −3.14 ppm (s, 24H; Al(CH$_3$)$_4$); ^{13}C{^{1}H} NMR (126 MHz, [D$_6$]benzene, 25°C): δ = 129.5, 122.3, 110.4 (Cp), 21.8 (CH$_3$), 15.2 (CH$_3$), 0.4 (Si(CH$_3$)$_3$), −20.9 ppm (brs; Al(CH$_3$)$_4$); IR (Nujol): $\tilde{\nu}$ = 1462 (vs, Nujol), 1383 (vs, Nujol), 1328 (m), 1256 (s), 1190 (m), 1030 (w), 964 (w), 842 (s), 765 (m), 732 (s), 583 (m), 555 (w), 517 cm^{-1} (w); elemental analysis calcd (%) for C$_{20}$H$_{45}$Al$_2$SiSm (517.99): C 46.38, H 8.76; found: C 46.43, H 8.87.

[Nd(AlMe$_4$)$_2$(C$_5$Me$_4$SiMe$_3$)] (3d): Following the procedure described above, [Nd(AlMe$_4$)$_3$] (**1d**) (410 mg, 1.01 mmol) and [C$_5$HMe$_4$SiMe$_3$] (196 mg, 1.01 mmol) yielded **3d** (389 mg, 0.76 mmol, 75%) as dark-blue crystals. ^{1}H NMR (500 MHz, [D$_6$]benzene, 25°C): δ = 14.74 (s, 6H; CH$_3$), 8.86 (s, 6H; CH$_3$), 5.25 (brs, 24H; Al(CH$_3$)$_4$), −3.09 ppm (s, 9H; Si(CH$_3$)$_3$); ^{13}C{^{1}H} NMR (126 MHz, [D$_6$]benzene, 25°C): δ = 240.1 (Cp), 236.3 (brs; Al(CH$_3$)$_4$), 131.5 (Cp), 8.99 (Si(CH$_3$)$_3$), −10.9 (CH$_3$), −20.6 ppm (CH$_3$); IR (Nujol): $\tilde{\nu}$ = 1453 (vs, Nujol), 1375 (vs, Nujol), 1328 (m), 1251 (s), 1199 (m), 1018 (w), 976 (w), 842 (s), 764 (m), 728 (s), 702 (s), 629 (w), 588 (m), 526 cm^{-1} (w); elemental analysis calcd (%) for C$_{20}$H$_{45}$Al$_2$SiNd (511.87): C 46.93, H 8.86; found: C 46.59, H 8.47.

[La(AlMe$_4$)$_2$(C$_5$Me$_4$SiMe$_3$)] (3e): Following the procedure described above, [La(AlMe$_4$)$_3$] (**1e**) (184 mg, 0.46 mmol) and [C$_5$HMe$_4$SiMe$_3$] (89 mg, 0.46 mmol) yielded **3e** (228 mg, 0.45 mmol, 98%) as colorless crystals. ^{1}H NMR (500 MHz, [D$_6$]benzene, 25°C): δ = 2.08 (s, 6H; CH$_3$), 1.79 (s, 6H; CH$_3$), 0.23 (s, 9H; Si(CH$_3$)$_3$), −0.25 ppm (s, 24H; Al(CH$_3$)$_4$); ^{13}C{^{1}H} NMR (126 MHz, [D$_6$]benzene, 25°C): δ = 134.0, 130.2, 122.8 (Cp), 15.0 (CH$_3$), 11.8 (CH$_3$), 2.4 (brs; Al(CH$_3$)$_4$), 2.2 ppm (Si(CH$_3$)$_3$); IR (Nujol): $\tilde{\nu}$ = 1468 (vs, Nujol), 1375 (vs, Nujol), 1323 (m), 1256 (s), 1214 (w), 1194 (m), 1126 (w), 1028 (w), 966 (w), 842 (s), 759 (m), 733 (s), 702 (s), 629 (w), 593 (m), 547 (w), 521 cm^{-1} (w); elemental analysis calcd (%) for C$_{20}$H$_{45}$Al$_2$SiLa (506.54): C 47.42, H 8.95; found: C 47.90, H 8.67.

General procedure for the preparation of [Ln(AlMe$_4$)$_2${1,2,4-(Me$_3$C)$_3$C$_5$H$_2$}] (4): In a glovebox, [Ln(AlMe$_4$)$_3$] (**1**) was dissolved in toluene (2 mL), and then a solution of [1,2,4-(Me$_3$C)$_3$C$_5$H$_3$] (1 equiv) in toluene (2 mL) was added to the alkylaluminate solution. The reaction mixture was transferred to a pressure tube and stirred for 24 h at 100°C. Upon cooling, the solvent was removed in vacuo to give compounds **4** as waxy solids. Crystallization from a solution in hexane at −35°C gave good yields of single crystals of **4** suitable for X-ray diffraction analysis.

[Sm(AlMe$_4$)$_2${1,2,4-(Me$_3$C)$_3$C$_5$H$_2$}] (4c): Following the procedure described above, [Sm(AlMe$_4$)$_3$] (**1c**) (371 mg, 0.90 mmol) and [1,2,4-(Me$_3$C)$_3$C$_5$H$_3$] (211 mg, 0.90 mmol) yielded **4c** (401 mg, 0.72 mmol, 80%) as red crystals. ^{1}H NMR (600 MHz, [D$_6$]benzene, 25°C): δ = 11.39 (brs, 2H; CpH), 0.93 (s, 18H; C(CH$_3$)$_3$), 0.22 (s, 9H; C(CH$_3$)$_3$), −2.76 (brs, 24H; Al(CH$_3$)$_4$); ^{13}C{^{1}H} NMR (151 MHz, [D$_6$]benzene, 25°C): δ = 136.6, 134.5, 112.2 (Cp), 37.7 (*C*(CH$_3$)$_3$), 35.9 (C(*C*H$_3$)$_3$), 31.6 (*C*(CH$_3$)$_3$), 28.7 ppm (C(*C*H$_3$)$_3$); IR (Nujol): $\tilde{\nu}$ = 1461 (vs, Nujol), 1372 (vs, Nujol), 1306 (w), 1234 (m), 1185 (m), 1024 (w), 1002 (w), 953 (w), 842 (m), 815 (w), 699 (s), 588 (m), 555 (m), 511 cm^{-1} (w); elemental analysis calcd (%) for C$_{25}$H$_{53}$Al$_2$Sm (558.02): C 53.81, H 9.57; found: C 54.12, H 9.91.

[Nd(AlMe$_4$)$_2${1,2,4-(Me$_3$C)$_3$C$_5$H$_2$}] (4d): Following the procedure described above, [Nd(AlMe$_4$)$_3$] (**1d**) (304 mg, 0.75 mmol) and [1,2,4-(Me$_3$C)$_3$C$_5$H$_3$] (176 mg, 0.75 mmol) yielded **4d** (265 mg, 0.48 mmol, 64%) as blue crystals. ^{1}H NMR (600 MHz, [D$_6$]benzene, 25°C): δ = 6.40 (brs, 24H; Al(CH$_3$)$_4$), 4.26 (brs, 2H; CpH), −0.81 (s, 18H; C(CH$_3$)$_3$), −1.03 ppm (s, 9H; C(CH$_3$)$_3$); ^{13}C{^{1}H} NMR (151 MHz, [D$_6$]benzene, 25°C): δ = 282.6, 263.0 (Cp), 239.5 (brs; Al(CH$_3$)$_4$), 235.9 (Cp), 55.0, 53.2 (C(*C*H$_3$)$_3$), 7.3, 6.5 ppm (*C*(CH$_3$)$_3$); IR (Nujol): $\tilde{\nu}$ = 1468 (vs, Nujol), 1375 (vs, Nujol), 1303 (w), 1235 (m), 1194 (m), 1163 (w), 1002 (w), 956 (w), 837 (m), 723 (s), 692 (s), 583 (m), 547 (m), 510 cm^{-1} (w); elemental analysis calcd (%) for C$_{25}$H$_{53}$Al$_2$Nd (551.90): C 54.41, H 9.68; found: C 54.44, H 9.84.

[La(AlMe$_4$)$_2${1,2,4-(Me$_3$C)$_3$C$_5$H$_2$}] (4e): Following the procedure described above, [La(AlMe$_4$)$_3$] (**1e**) (424 mg, 1.06 mmol) and [1,2,4-

$(Me_3C)_3C_5H_3$] (249 mg, 1.06 mmol) yielded **4e** (359 mg, 0.66 mmol, 62%) as colorless crystals. ^{1}H NMR (600 MHz, [D$_6$]benzene, 25°C): $\delta = 6.28$ (s, 2H; CpH), 1.31 (s, 18H; C(CH$_3$)$_3$), 1.15 (s, 9H; C(CH$_3$)$_3$), −0.12 ppm (s, 24H; Al(CH$_3$)$_4$); ^{13}C{^{1}H} NMR (151 MHz, [D$_6$]benzene, 25°C): $\delta = 144.4$, 142.7, 116.9 (Cp), 34.5 (*C*(CH$_3$)$_3$), 33.9 (C(*C*H$_3$)$_3$), 33.3 (*C*(CH$_3$)$_3$), 31.8 (C(*C*H$_3$)$_3$), 3.2 ppm (brs; Al(CH$_3$)$_4$); IR (Nujol): $\tilde{\nu} = 1466$ (vs, Nujol), 1378 (vs, Nujol), 1300 (w), 1245 (m), 1196 (m), 1168 (w), 1030 (w), 1002 (w), 958 (w), 914 (w), 892 (w), 837 (m), 721 (s), 699 (s), 577 (m), 550 (m), 511 cm^{-1} (w); elemental analysis calcd (%) for $C_{25}H_{53}Al_2La$ (546.57): C 54.94, H 9.77; found: C 54.72, H 9.96.

[{Y(AlMe$_4$)(μ-Cl){1,3-(Me$_3$Si)$_2$C$_5$H$_3$}}$_2$] (6): In a glovebox, [Y(AlMe$_4$)$_2$-{1,3-(Me$_3$Si)$_2$C$_5$H$_3$}] (**2b**) (85 mg, 0.18 mmol) was dissolved in hexane (3 mL) and Me$_2$AlCl (180 μL, 0.18 mmol) was added. The reaction mixture was stirred for 5 min and then cooled to −35°C. Colorless single crystals of **6** (30 mg, 0.04 mmol, 40%) suitable for X-ray diffraction analysis were harvested after 7 d. ^{1}H NMR (600 MHz, [D$_6$]benzene, 25°C): $\delta = 6.89$ (s, 2H; CpH), 6.81 (d, $^3J = 2.4$ Hz, 4H; CpH), 0.27 (s, 36H; Si(CH$_3$)$_3$), −0.11 ppm (d, $^2J_{YH} = 2.4$ Hz, 24H; Al(CH$_3$)$_4$); ^{13}C{^{1}H} NMR (151 MHz, [D$_6$]benzene, 25°C): $\delta = 131.1$, 130.5, 126.1 (Cp), 2.09 (brs; Al(CH$_3$)$_4$), 0.48 ppm (Si(CH$_3$)$_3$); elemental analysis calcd (%) for $C_{30}H_{66}Cl_2Al_2Si_4Y_2$ (841.88): C 42.80, H 7.90; found: C 43.08, H 8.02.

[{YCl$_2${1,3-(Me$_3$Si)$_2$C$_5$H$_3$}}$_n$] (7): In a glovebox, [Y(AlMe$_4$)$_2$-{1,3-(Me$_3$Si)$_2$C$_5$H$_3$}] (**2b**) (132 mg, 0.28 mmol) was dissolved in hexane (3 mL) and excess Me$_2$AlCl was added. The reaction mixture was stirred for 16 h at ambient temperature and then cooled to −35°C. Compound **7** (31 mg, 0.08 mmol, 30%) was obtained as a white powdery solid after 2 d. ^{1}H NMR (600 MHz, [D$_6$]benzene, 25°C): $\delta = 7.18$ (s, 1H; CpH), 7.05 (d, $^3J = 1.8$ Hz, 2H; CpH), 0.50 ppm (s, 18H; Si(CH$_3$)$_3$); ^{13}C{^{1}H} NMR (151 MHz, [D$_6$]benzene, 25°C): $\delta = 132.1$, 131.7, 126.1 (Cp), 0.65 ppm (Si(CH$_3$)$_3$).

[{Y(AlMe$_4$)(μ-Cl)(C$_5$Me$_4$SiMe$_3$)}$_2$] (8): In a glovebox, [Y(AlMe$_4$)$_2$(C$_5$Me$_4$SiMe$_3$)] (**3b**) (105 mg, 0.23 mmol) was dissolved in hexane (3 mL) and Me$_2$AlCl (230 μL, 0.23 mmol) was added. The reaction mixture was stirred for 5 min and then cooled to −35°C. Colorless single crystals of **8** (38 mg, 0.05 mmol, 41%) suitable for X-ray diffraction analysis were harvested after 2 d. ^{1}H NMR (500 MHz, [D$_6$]benzene, 25°C): $\delta =$ 2.08 (s, 12H; CH$_3$), 1.81 (s, 12H; CH$_3$), 0.31 (s, 18H; Si(CH$_3$)$_3$), −0.20 (d, $^2J_{YH} = 2.0$ Hz, 24H; Al(CH$_3$)$_4$); ^{13}C{^{1}H} NMR (126 MHz, [D$_6$]benzene, 25°C): $\delta = 129.5$, 127.4, 118.7 (Cp), 15.0 (CH$_3$), 11.9 (CH$_3$), 2.1 (Si(CH$_3$)$_3$), 0.2 ppm (brs; Al(CH$_3$)$_4$); elemental analysis calcd (%) for $C_{32}H_{66}Al_2Cl_2Si_2Y_2$ (809.73): C 47.47, H 8.22; found: C 47.83, H 8.30.

[{Nd(AlMe$_4$)(μ-Cl)-{1,2,4-(Me$_3$C)$_3$C$_5$H$_2$}}$_2$] (9): In a glovebox, [Nd(AlMe$_4$)$_2${1,2,4-(Me$_3$C)$_3$C$_5$H$_2$}] (**4d**) (33 mg, 0.06 mmol) was dissolved in hexane (3 mL) and Me$_2$AlCl (60 μL, 0.06 mmol) was added. The reaction mixture was stirred for 5 min and then cooled to −35°C. Blue single crystals of **9** (10 mg, 0.01 mmol, 35%) suitable for X-ray diffraction analysis were harvested after 7 d. ^{1}H NMR (600 MHz, [D$_6$]benzene, 25°C): $\delta = 9.63$ (brs, 24H; Al(CH$_3$)$_4$), 0.88 (brs, 4H; CpH), −0.58 (s, 18H; C(CH$_3$)$_3$), −3.80 ppm (s, 36H; C(CH$_3$)$_3$); ^{13}C{^{1}H} NMR (151 MHz, [D$_6$]benzene, 25°C): $\delta =$ 282.4, 262.7 (Cp), 211.1 (brs; Al(CH$_3$)$_4$), 235.7 (Cp), 54.9, 53.1 (C(*C*H$_3$)$_3$), 7.2, 6.3 ppm (*C*(CH$_3$)$_3$); elemental analysis calcd (%) for $C_{42}H_{82}Al_2Cl_2Nd_2$ (1000.46): C 50.42, H 8.26; found: C 50.73, H 8.57.

Polymerization of isoprene: A detailed polymerization procedure (run 12, Table 5) is described as a typical example. B(C$_6$F$_5$)$_3$ (10 mg, 0.02 mmol, 1 equiv) was added to a solution of **3e** (9 mg, 0.02 mmol) in toluene (8 mL) and the mixture was aged at ambient temperature for 15 min. After the addition of isoprene (2.0 mL, 20 mmol), polymerization was carried out at 40°C for 24 h. The polymerization mixture was poured into a large quantity of acidified isopropanol containing 0.1% (w/w) 2,6-di-*tert*-butyl-4-methylphenol as a stabilizer. The polymer was washed with isopropanol and dried under vacuum at ambient temperature to constant weight. The polymer yield was determined gravimetrically.

Single-crystal X-ray structures: Crystal data and details of the structure determination are presented in Tables 6 and 7. Single crystals were placed in a nylon loop containing Paratone oil (Hampton Research) under argon atmosphere, and then mounted directly into the N_2 cold stream (Oxford Cryosystems Series 700) on a Bruker AXS SMART 2 K CCD diffractometer. Data were collected by means of 0.3–0.4° ω scans in four orthogonal ϕ settings using $Mo_{K\alpha}$ radiation ($\lambda = 0.71073$ Å) and a fifth and final partial run to evaluate crystal decay. Data collection was controlled using the program SMART,[37] data integration was performed with SAINT,[37] and structure solution and model refinement were carried out with SHELXS-97 and SHELXL-97.[38]

All data sets were subjected to face indexed based numerical absorption correction,[39] except for the data sets for **2a** and **3b**, which were corrected using multi-abs methods.[40]

Non-coordinating methyl groups were refined as rigid and rotating (difference Fourier density optimization) about the respective Al–C bonds. Coordinating methyl groups were refined as rigid pyramidal groups with the same C–H and H···H distances as in the previous case, but with the threefold axis of the pyramidal rigid group allowed to be non-parallel

Table 6. Crystallographic data for compounds **2a**, **2b**, **2d**, and **3b**.

	2a	**2b**	**2d**	**3b**
formula	$C_{19}H_{45}Al_2Si_2Lu$	$C_{19}H_{45}Al_2Si_2Y$	$C_{19}H_{45}Al_2Si_2Nd$	$C_{20}H_{45}Al_2SiY$
Fw	558.66	472.60	527.93	456.52
color/habit	colorless/plate	colorless/needle	blue/needle	colorless/prism
crystal dimensions [mm^3]	0.58×0.38×0.10	0.38×0.08×0.06	0.48×0.15×0.08	0.30×0.25×0.21
crystal system	monoclinic	monoclinic	monoclinic	monoclinic
space group	$P2_1/m$	$P2_1/m$	$P2_1/m$	$P2_1/n$
a [Å]	9.7232(2)	9.6386(7)	9.5762(2)	10.1774(2)
b [Å]	14.1302(4)	14.182(1)	14.1496(3)	13.4321(3)
c [Å]	9.8051(2)	9.9401(7)	10.1438(2)	19.0942(4)
α [°]	90	90	90	90
β [°]	101.5063(4)	100.792(1)	98.94(1)	105.036(1)
γ [°]	90	90	90	90
V [Å^3]	1320.1(1)	1334.7(2)	1357.77(5)	2520.88(9)
Z	2	2	2	4
T [K]	103	123	123	123
ρ_{calcd} [mg m^{-3}]	1.406	1.176	1.291	1.203
μ [mm^{-1}]	3.897	2.341	2.066	2.432
F(000)	568	504	546	976
θ range [°]	2.14/30.11	2.09/25.56	2.15/30.12	1.88/32.07
index ranges	$-13 \le h \le 13$	$-11 \le h \le 11$	$-13 \le h \le 13$	$-15 \le h \le 14$
	$-19 \le k \le 19$	$-17 \le k \le 17$	$-19 \le k \le 19$	$-20 \le k \le 20$
	$-13 \le l \le 13$	$-12 \le l \le 12$	$-12 \le l \le 14$	$-24 \le l \le 28$
no. of reflns. integrated	22357	16035	17306	35693
no. of indep. reflns./R_{int}	4035/0.0200	2599/0.0415	4137/0.0143	8728/0.0226
no. of obsd. reflns. ($I > 2\sigma(I)$)	3957	2275	4001	7642
data/params./restraints	4035/142/21	2599/142/12	4137/148/21	8728/256/18
$R1$/$wR2$ ($I > 2\sigma(I)$)[a]	0.0108/0.0279	0.0249/0.0587	0.0161/0.0406	0.0237/0.0596
$R1$/$wR2$ (all data)[a]	0.0112/0.0281	0.0343/0.0623	0.0168/0.0410	0.0311/0.0625
GOF (on F^2)[a]	1.089	1.055	1.071	1.047
largest diff. peak and hole [e Å^{-3}]	0.494/−0.648	0.343/−0.304	1.399/−0.446	0.534/−0.639

[a] $R1 = \Sigma(||F_0| - |F_c||)/\Sigma|F_0|$; $wR2 = \{\Sigma[w(F_0^2 - F_c^2)^2]/\Sigma[w(F_0^2)^2]\}^{1/2}$; GOF $= \{\Sigma[w(F_0^2 - F_c^2)^2]/(n-p)\}^{1/2}$.

Table 7. Crystallographic data for compounds **4c**, **4d**, **4e**, **8**, and **9**.

	4c	**4d**	**4e**	**8**	**9**
formula	$C_{25}H_{53}Al_2Sm$	$C_{25}H_{53}Al_2Nd$	$C_{25}H_{53}Al_2La$	$C_{32}H_{66}Cl_2Al_2Si_2Y_2$	$C_{42}H_{82}Cl_2Al_2Nd_2$
Fw	557.98	551.87	546.54	809.70	1000.42
color/habit	red/prism	blue/irregular prism	colorless/prism	colorless/prism	blue/needle
crystal dimensions [mm^3]	$0.48\times0.25\times0.22$	$0.62\times0.42\times0.30$	$0.48\times0.45\times0.35$	$0.25\times0.15\times0.05$	$0.32\times0.06\times0.03$
crystal system	triclinic	orthorhombic	orthorhombic	monoclinic	triclinic
space group	$P\bar{1}$	$P2_12_12_1$	$P2_12_12_1$	$P2_1/c$	$P\bar{1}$
a [Å]	10.4475(3)	9.9821(3)	10.0116(3)	12.2263(4)	9.6135(4)
b [Å]	11.5594(3)	16.3710(5)	16.4193(5)	18.3134(6)	11.6331(5)
c [Å]	12.6169(3)	18.4738(6)	18.5254(5)	9.5255(3)	11.8715(5)
α [°]	98.9720(4)	90	90	90	70.350(1)
β [°]	97.1495(4)	90	90	96.228(1)	75.971(1)
γ [°]	96.1548(1)	90	90	90	88.487(1)
V [Å^3]	1480.84(7)	3018.9(2)	3045.3(2)	2120.2(1)	1210.83(9)
Z	2	4	4	2	1
T [K]	123	123	123	123	123
ρ_{calcd} [mg m^{-3}]	1.251	1.214	1.192	1.268	1.372
μ [mm^{-1}]	2.050	1.786	1.468	2.966	2.292
$F(000)$	582	1156	1144	848	514
θ range [°]	1.65/30.02	2.32/30.04	2.20/30.12	1.68/29.05	2.15/27.02
index ranges	$-14\le h\le14$	$-14\le h\le14$	$-14\le h\le14$	$-16\le h\le16$	$-12\le h\le12$
	$-16\le k\le16$	$-23\le k\le23$	$-23\le k\le23$	$-25\le k\le24$	$-14\le k\le14$
	$-17\le l\le17$	$-26\le l\le26$	$-26\le l\le26$	$-13\le l\le12$	$-15\le l\le15$
no. of reflns. integrated	25046	51098	51756	33224	16676
no. of indep. reflns./R_{int}	8638/0.0135	8806/0.0203	8960/0.0189	5652/0.0316	5294/0.0302
no. of obsd. reflns ($I>2\sigma(I)$)	8366	8294	8729	4750	4767
data/params./restraints	8638/302/24	8806/302/24	8960/302/24	5652/208/12	5294/246/12
$R1$/$wR2$ ($I>2\sigma(I)$)[a]	0.0168/0.0442	0.0176/0.0410	0.0131/0.0338	0.0240/0.0559	0.0202/0.0437
$R1$/$wR2$ (all data)[a]	0.0174/0.0446	0.0209/0.0430	0.0140/0.0343	0.0346/0.0603	0.0259/0.0457
GOF (on F^2)[a]	1.076	1.068	1.027	1.042	1.032
largest diff. peak and hole [e Å^{-3}]	3.018/−0.585	0.750/−0.456	0.524/−0.412	1.186/−0.608	0.473/−0.366

[a] $R1=\Sigma(||F_o|-|F_c||)/\Sigma|F_o|$; $wR2=\{\Sigma[w(F_o^2-F_c^2)^2]/\Sigma[w(F_o^2)^2]\}^{1/2}$; GOF $=\{\Sigma[w(F_o^2-F_c^2)^2]/(n-p)\}^{1/2}$.

with the C−Al bond axis. The isotropic displacement parameters for all methyl H-atoms were set at 1.5 times that of the pivot C-atom.

CCDC-653204, 653205, 679299, 679300, 679301, 679302, 679303, 679304, and 679305 contain the supplementary crystallographic data for this paper. These data can be obtained free of charge from the Cambridge Crystallographic Data Centre via www.ccdc.cam.ac.uk/data_request/cif.

Acknowledgements

Financial support from the Norwegian Research Council (Project No. 182547/I30) and the program Nanoscience@UiB is gratefully acknowledged. We also thank Till Diesing (c/o Dr. Markus Klapper, MPI für Polymerforschung, Mainz (Germany)) for performing the GPC analyses.

[1] a) K. C. Hultzsch, T. P. Spaniol, J. Okuda, *Angew. Chem.* **1999**, *111*, 163; *Angew. Chem. Int. Ed.* **1999**, *38*, 227; b) Y. Luo, J. Baldamus, Z. Hou, *J. Am. Chem. Soc.* **2004**, *126*, 13910; c) X. Li, J. Baldamus, Z. Hou, *Angew. Chem.* **2005**, *117*, 984; *Angew. Chem. Int. Ed.* **2005**, *44*, 962; d) D. Cui, M. Nishiura, Z. Hou, *Macromolecules* **2005**, *38*, 4089; e) J. Hitzbleck, J. Okuda, *Z. Anorg. Allg. Chem.* **2006**, *632*, 1947; f) J. Hitzbleck, K. Beckerle, J. Okuda, T. Halbach, R. Mühlhaupt, *Macromol. Symp.* **2006**, *236*, 23; g) H. Zhang, Y. Luo, Z. Hou, *Macromolecules* **2008**, *41*, 1064.

[2] a) S. Bambirra, D. van Leusen, A. Meetsma, B. Hessen, J. H. Teuben, *Chem. Commun.* **2003**, 522; b) S. Bambirra, M. W. Bouwkamp, A. Meetsma, B. Hessen, *J. Am. Chem. Soc.* **2004**, *126*, 9182; c) W. P. Kretschmer, A. Meetsma, B. Hessen, T. Schmalz, S. Qayyum, R. Kempe, *Chem. Eur. J.* **2006**, *12*, 8969; d) S. Bambirra, D. van Leusen, C. G. J. Tazelaar, A. Meetsma, B. Hessen, *Organometallics* **2007**, *26*, 1014; e) Y. Luo, M. Nishiura, Z. Hou, *J. Organomet. Chem.* **2007**, *692*, 536; f) Y. Yang, B. Liu, W. Gao, D. Cui, X. Chen, X. Jing, *Organometallics* **2007**, *26*, 4575; g) S. Li, W. Miao, T. Tang, W. Dong, X. Zhang, D. Cui, *Organometallics* **2008**, *27*, 718; h) A. Otero, J. Fernández-Baeza, A. Antinolo, A. Lara-Sánchez, E. Martínez-Caballero, J. Tejeda, L. F. Sánchez-Barba, C. Alonso-Moreno, I. López-Solera, *Organometallics* **2008**, *27*, 976.

[3] a) X. Liu, X. Shang, T. Tang, N. Hu, F. Pei, D. Cui, X. Chen, X. Jing, *Organometallics* **2007**, *26*, 2747; b) D. J. H. Emslie, W. E. Piers, M. Parvez, R. McDonald, *Organometallics* **2002**, *21*, 4226.

[4] a) L. Zhang, T. Suzuki, Y. Luo, M. Nishiura, Z. Hou, *Angew. Chem.* **2007**, *119*, 1941; *Angew. Chem. Int. Ed.* **2007**, *46*, 1909; b) B. Liu, D. Cui, J. Ma, X. Chen, X. Jing, *Chem. Eur. J.* **2007**, *13*, 834.

[5] a) X. Li, M. Nishiura, K. Mori, T. Mashiko, Z. Hou, *Chem. Commun.* **2007**, 4137; b) F. Jaroschik, T. Shima, X. Li, K. Mori, L. Ricard, X.-F. Le Goff, F. Nief, Z. Hou, *Organometallics* **2007**, *26*, 5654.

[6] L. Zhang, Y. Luo, Z. Hou, *J. Am. Chem. Soc.* **2005**, *127*, 14562.

[7] R. Anwander, M. G. Klimpel, H. M. Dietrich, D. J. Shorokhov, W. Scherer, *Chem. Commun.* **2003**, 1008.

[8] H. M. Dietrich, C. Zapilko, E. Herdtweck, R. Anwander, *Organometallics* **2005**, *24*, 5767.

[9] M. Zimmermann, N. Å. Frøystein, A. Fischbach, P. Sirsch, H. M. Dietrich, K. W. Törnroos, E. Herdtweck, R. Anwander, *Chem. Eur. J.* **2007**, *13*, 8784.

[10] E. Le Roux, F. Nief, F. Jaroschik, K. W. Törnroos, R. Anwander, *Dalton Trans.* **2007**, 4866.

[11] H. M. Dietrich, E. Herdtweck, K. W. Törnroos, R. Anwander, unpublished results.

[12] W. T. Klooster, R. S. Lu, R. Anwander, W. J. Evans, T. E. Koetzle, R. Bau, *Angew. Chem.* **1998**, *110*, 1326; *Angew. Chem. Int. Ed.* **1998**, *37*, 1268.

[13] M. Zimmermann, K. W. Törnroos, R. Anwander, *Angew. Chem.* **2007**, *119*, 3187; *Angew. Chem. Int. Ed.* **2007**, *46*, 3126.

[14] H. M. Dietrich, O. Schuster, K. W. Törnroos, R. Anwander, *Angew. Chem.* **2006**, *118*, 4977; *Angew. Chem. Int. Ed.* **2006**, *45*, 4858.
[15] Catalyst deactivation is observed in the presence of excessive amounts of coordinating solvents. For examples, see: a) L. Friebe, O. Nuyken, W. Obrecht, *Adv. Polym. Sci.* **2006**, *204*, 1; b) P. G. Hayes, W. E. Piers, M. Parvez, *J. Am. Chem. Soc.* **2003**, *125*, 5622.
[16] It is noteworthy that for a considerable number of binary catalysts $[Ln^{III}(Do)(\mathbf{L})R_2]$/borate the presence of organoaluminum compounds such as $Al(i\mathrm{Bu})_3$ is required; for examples, see refs. [1e], [1f], [2a–c], [2f].
[17] A. Fischbach, R. Anwander, *Adv. Polym. Sci.* **2006**, *204*, 155.
[18] A. Fischbach, M. G. Klimpel, M. Widenmeyer, E. Herdtweck, W. Scherer, R. Anwander, *Angew. Chem.* **2004**, *116*, 2284; *Angew. Chem. Int. Ed.* **2004**, *43*, 2234.
[19] C. Meermann, K. W. Törnroos, W. Nerdal, R. Anwander, *Angew. Chem.* **2007**, *119*, 6628; *Angew. Chem. Int. Ed.* **2007**, *46*, 6508.
[20] a) A. Fischbach, F. Perdih, P. Sirsch, W. Scherer, R. Anwander, *Organometallics* **2002**, *21*, 4569; b) A. Fischbach, F. Perdih, E. Herdtweck, R. Anwander, *Organometallics* **2006**, *25*, 1626; c) A. Fischbach, C. Meermann, G. Eickerling, W. Scherer, R. Anwander, *Macromolecules* **2006**, *39*, 6811.
[21] a) M. Zimmermann, K. W. Törnroos, R. Anwander, *Organometallics* **2006**, *25*, 3593; b) M. Zimmermann, F. Estler, E. Herdtweck, K. W. Törnroos, R. Anwander, *Organometallics* **2007**, *26*, 6029; c) M. Zimmermann, J. Takats, G. Kiel, K. W. Törnroos, R. Anwander, *Chem. Commun.* **2008**, 612.
[22] M. Zimmermann, K. W. Törnroos, R. Anwander, *Angew. Chem.* **2008**, *120*, 787; *Angew. Chem. Int. Ed.* **2008**, *47*, 775.
[23] The contents of this contribution have been presented at the XX. Tage der Seltenen Erden "Terrae Rarae 2007", Köln (Bonn-Röttgen), Germany, 29.11.–1.12.2007.
[24] E. W. Abel, S. Moorhouse, *J. Organomet. Chem.* **1971**, *29*, 227.
[25] After submission of this work, the synthesis of complexes **3** and the catalytic performance of mixtures **3**/$[Ph_3C][B(C_6F_5)_4]$/$Al(i\mathrm{Bu})_3$ in the polymerization of butadiene was reported, see: D. Robert, T. P. Spaniol, J. Okuda, *Eur. J. Inorg. Chem.* **2008**, 2801.
[26] a) E. V. Dehmlow, C. Bollmann, *Z. Naturforsch.* **1993**, *48b*, 457; b) H. Sitzmann, P. Zhou, G. Wolmershäuser, *Chem. Ber.* **1994**, *127*, 3.
[27] a) M. G. Schrems, H. M. Dietrich, K. W. Törnroos, R. Anwander, *Chem. Commun.* **2005**, 5922; b) H.-M. Sommerfeldt, C. Meermann, M. G. Schrems, K. W. Törnroos, N. Å. Frøystein, R. J. Miller, E.-W. Scheidt, W. Scherer, R. Anwander, *Dalton Trans.* **2008**, 1899.
[28] C. Ruspic, J. R. Moss, M. Schürmann, S. Harder, *Angew. Chem.* **2008**, *120*, 2151; *Angew. Chem. Int. Ed.* **2008**, *47*, 2121.
[29] M. Zimmermann, K. W. Törnroos, R. Anwander, unpublished results.
[30] Alternative treatment with one equivalent of Ph_3CCl as chlorinating agent also yielded compounds **6**, **8**, and **9**.
[31] For an example of a half-sandwich bis(chloride) rare-earth metal complex, see: M. D. Walter, D. Bentz, F. Weber, O. Schmitt, G. Wolmershäuser, H. Sitzmann, *New J. Chem.* **2007**, *31*, 305.
[32] W. J. Evans, R. Anwander, J. W. Ziller, *Organometallics* **1995**, *14*, 1107.
[33] D. Barbier-Baudry, F. Bonnet, B. Domenichini, A. Dormond, M. Visseaux, *J. Organomet. Chem.* **2004**, *647*, 167.
[34] a) F. Bonnet, M. Visseaux, A. Pereira, F. Bouyer, D. Barbier-Baudry, *Macromol. Rapid Commun.* **2004**, *25*, 873; b) F. Bonnet, M. Visseaux, D. Barbier-Baudry, E. Vigier, M. M. Kubicki, *Chem. Eur. J.* **2004**, *10*, 2428; c) F. Bonnet, M. Visseaux, A. Pereira, D. Barbier-Baudry, *Macromolecules* **2005**, *38*, 3162.
[35] For *trans*-1,4 polymerization of isoprene by $NdCl_3$ catalysts, see: a) J. H. Yang, M. Tsutsui, Z. Chen, D. E. Bergbreiter, *Macromolecules* **1982**, *15*, 230; b) Y. B. Monakov, Z. M. Sabirov, V. N. Urazbaev, V. P. Efimov, *Kinet. Catal.* **2001**, *42*, 310.
[36] The reaction of $[La(AlMe_4)_2(C_5Me_5)]$ and $B(C_6F_5)_3$ was shown to quantitatively produce the ion pair $[\{[La(C_5Me_5)\{(\mu\text{-}Me)_2AlMe(C_6F_5)\}][Me_2Al(C_6F_5)_2]\}_2]$ as the product of very fast sequential CH_3/C_6F_5 exchange processes. A similar initial activation scenario can be proposed for other half-sandwich bis(aluminate) complexes (see ref. [22]).
[37] SMART, Ver. 5.054, **1999** and SAINT, Ver. 6.45a, Bruker AXS Inc., Madison, Wisconsin (USA), **2001**.
[38] G. M. Sheldrick, *Acta Crystallographica, A64*, **2008**, 112.
[39] SHELXTL, Ver. 6.14, Bruker AXS Inc., Madison, Wisconsin (USA), **2003**.
[40] G. M. Sheldrick, SADABS, Ver. 2004/1, University of Göttingen (Germany), **2006**.

Received: March 16, 2008
Published online: July 4, 2008

